Anomalous exponents and dipole solutions for the thin film equation

M. Bowen, J. Hulshof and J. R. King

M. Bowen, Department of Mathematics, Duke University, Durham, NC 27708-0320, U.S.A.

J. Hulshof, Division of Mathematics and Computer Science, Free University Amsterdam

De Boelelaan 1081, 1081 HV Amsterdam, The Netherlands

`http://www.cs.vu.nl/~jhulshof/PAPERS/37.ps`

J. R. King, Division of Theoretical Mechanics, University of Nottingham

University ParK, Nottingham NG7 2RD, United Kingdom

AMS subject classifications: 35K65, 34E05, 34A34

Key words: thin film equation, 4-dimensional phase space,

asymptotic expansions, self-similarity, numerics

Abbreviated title: Anomalous dipole solutions for the thin film equation

Abstract

We investigate similarity solutions of the 'thin film' equation. In particular we look at solutions on the half-line $x \geq 0$ with compact support and zero contact angle boundary conditions in $x = 0$. Such 'dipole' solutions feature an anomalous exponent and are therefore called similarity solutions of the second kind. Using a combination of phase space analysis and numerical simulations, we numerically construct trajectories representing these solutions, at the same time obtaining broader insight into the nature of the four-dimensional phase space. Additional asymptotic analysis provides further information concerning the evolution to self-similarity.

1 Introduction

In this paper we continue the study of the asymptotic behaviour of (non-negative) solutions to the 'thin film' equation

$$\frac{\partial h}{\partial t} = -\frac{\partial}{\partial x}\left(|h|^n \frac{\partial^3 h}{\partial x^3}\right) \tag{1.1}$$

on the half-line $x > 0$.

Equation (1.1) arises in a number of physical contexts. Specific applications, with $h(x,t) \geq 0$ being the thickness of the fluid, include capillary driven Newtonian droplet spreading over a flat surface with no slip ($n = 3$, $y = 0$ being the rigid substrate and $y = h(x,t)$ the free surface), with Navier slip dominant ($n = 2$, cf. [1], for example, and Appendix 2), and in a Hele-Shaw cell ($n = 1$, e.g. [2]; the same exponent arises in the slip-dominated limit for the ad hoc slip law adopted in [3]). We note that in the relevant formulations the slip terms dominate for sufficiently small h, this being required for a contact line to advance. Further discussion of physical isssues relating to the boundary conditions outlined below and to the evolution equation is given in Appendix 1 and Appendix 2, respectively; our emphasis in the main body of the paper is in the development of a number of mathematical tools for the analysis of (1.1), and their application in combination to provide comprehensive understanding of a key initial-boundary value problem. We stress by way of mathematical motivation that much of even the qualitative behaviour of (1.1) remains open; moreover, it provides an important paradigm in the study of moving boundary problems for partial differential equations (PDE's) which lack a comparison principle, so that existing techniques (many of which were developed in studies of equation (1.2)) do not for the most part apply. We believe the current paper to represent the first detailed investigation of second kind phenomena (in the sense of second kind similarity reductions of the full PDE) in a diffusion equation of higher order; as such, it opens the way for the investigation of the many other effects which can also be described by second kind solutions (see [4] for their classification in the corresponding second-order equation, (1.2)).

From a mathematical point there are several perspectives on equation (1.1). At first glance it resembles the well-known porous medium equation, which in one dimension reads

$$\frac{\partial h}{\partial t} = \frac{\partial}{\partial x}\left(|h|^n \frac{\partial h}{\partial x}\right), \tag{1.2}$$

which occurs (see e.g. [5] and [4]) with different values of positive and negative n in many applications and which derives its name from its role in the description of flows in porous media, going back as far as [6]. The porous medium equation is a nonlinear degenerate version of the classical linear heat equation and its mathematical study has played a central part in the study of general nonlinear degenerate parabolic equations. For each $n > 0$ it has a family of exact self-similar compactly supported source type solutions which describe the large time behaviour of compactly supported (non-negative or sign changing) solutions with non-zero integral $\int h(x,t)dx$; this integral is a conserved quantity of the solution. In one dimension, solutions with zero integral and non-zero first moment $\int xh(x,t)dx$ have large time behaviour governed by a family of exact self-similar compactly supported dipole type solutions, see [7]; these solutions also describe the intermediate asymptotic behaviour of the semi-infinite domain $(x > 0)$ problem with $h = 0$ on $x = 0$.

In the light of the above it is natural to consider the thin film equation with n as a real parameter and there is by now a large literature on (1.1) with $n > 0$, see e.g. [8], [9] and the overview papers [10],[11],[12],[13]. The first thing to note is that the analogy between the porous medium equation and the thin film equation has only limited value. In fact, there is another fourth-order equation, namely

$$\frac{\partial h}{\partial t} = -\frac{\partial^3}{\partial x^3}\left(|h|^n \frac{\partial h}{\partial x}\right),$$

studied in [14], which has solutions behaving much more like solutions of the porous medium equation, the most notable difference being that solutions typically have infinitely many sign changes near the boundary of their support. This behaviour is uniform in $n > 0$ and there are no corresponding critical exponents.

The theory for (1.1) is much more complicated, the first striking observation being that self-similar compactly supported source type solutions exist only for $n < 3$; see [15]. We note that these solutions are positive on the interior of their support and that most studies of (1.1) restrict attention to non-negative solutions. This restriction is natural in view of the physical background but mathematically speaking is rather arbitrary. At the boundary of their support, the source type solutions in [15] have zero flux, i.e.

$$h^n \frac{\partial^3 h}{\partial x^3} = 0,$$

(so that, as in the case of the porous medium equation, the integral $\int h(x,t)dx$ is conserved) as well as zero contact angle, meaning that the first x-derivative of $h(x,t)$ vanishes at the free boundary. Such solutions are called strong solutions and one of the hardest open problems in the study of (1.1) is the uniqueness of strong solutions to the Cauchy problem. This is strongly related to the form of (1.1), which prohibits a straightforward definition of weak solutions via test functions and two integrations by parts. Our perspective is that for $n < 3$ non-negative strong solutions of (1.1) are solutions of a free boundary problem, with moving boundary conditions

$$h = \frac{\partial h}{\partial x} = h^n \frac{\partial^3 h}{\partial x^3} = 0 \quad \text{(zero contact angle and zero flux)}, \tag{1.3}$$

at the free boundary $x = s(t)$. Here $s(t)$ is the supremum of the spatial support of $h(x,t)$ and similar free boundary conditions have to be imposed at the infimum of the support. Note that the condition on the flux has to be read as

$$\lim_{x \uparrow s(t)} h^n \frac{\partial^3 h}{\partial x^3} = 0.$$

Solutions of this free boundary problem should then have a large time behaviour governed by the source-type solutions in [15]. There are however only partial results in this direction; see [16],[17],[18], another major additional difficulty being the absence of a comparison principle for fourth-order equations. In the free boundary perspective, the limit $n \to 0$ gives a free boundary problem for the linear equation

$$\frac{\partial h}{\partial t} = -\frac{\partial^4 h}{\partial x^4}, \tag{1.4}$$

with the spatial derivatives of order zero, one and three vanishing at the free boundary. In fact, compactly supported source type solutions of the free boundary formulation above exist for all $-4 < n < 3$; see [19],[20].

In the afterword of his book [21], Barenblatt calls for a study of (1.1) on the half-line $x > 0$, subject to, in addition to (1.3), appropriate conditions at $x = 0$. In [22] we have identified two natural choices, namely

$$h = \frac{\partial h}{\partial x} = 0 \quad \text{(zero contact angle)} \tag{1.5}$$

or

$$h = h^n \frac{\partial^3 h}{\partial x^3} = 0 \quad \text{(zero flux)}. \tag{1.6}$$

The case of zero flux boundary conditions at $x = 0$ combined with zero contact angle and zero flux free boundary conditions was analysed in [22]. The corresponding (first kind) self-similar solutions exist for the whole range $-4 < n < 3$. In the drainage context however, see Appendix

1, the zero contact angle condition at $x = 0$ is more natural and thus this paper deals mainly with the boundary conditions

$$\begin{aligned} h = \frac{\partial h}{\partial x} &= 0 \qquad \text{at } x = 0 \text{ and } x = s(t) \quad \text{(zero contact angle)}, \\ \lim_{x \uparrow s(t)} h^n \frac{\partial^3 h}{\partial x^3} &= 0 \qquad \text{at } x = s(t) \qquad \text{(zero flux)}. \end{aligned} \tag{1.7}$$

The (compactly supported) initial data are

$$\text{at } t = 0 \qquad h = h_0(x), \quad s = a, \tag{1.8}$$

in which $0 \le x \le a$.

It was shown in [22] that self-similar solutions of (1.1) satisfying (1.5) at $x = 0$ can exist only if $n < 2$. This restriction is needed for drainage of fluid over the edge $x = 0$ to be possible, in other words, to permit the flux

$$J(t) = -h^n \frac{\partial^3 h}{\partial x^3}\bigg|_{x=0} \tag{1.9}$$

to be positive, cf. Appendix 1. For $0 < n < 2$ one then expects the asymptotic behaviour of solutions to (1.1),(1.7),(1.8) as $t \to \infty$ to be given by a dipole type self-similar solution (see [21] for numerous other such examples), whereby

$$h \sim t^{-\alpha} f(x/t^{\beta}) \text{ as } t \to \infty \text{ with } x = O(t^{\beta}) \tag{1.10}$$

with (from (1.1))

$$n\alpha + 4\beta = 1. \tag{1.11}$$

Unlike in the mass conservation case, the 'anomalous' exponent α has to determined from a nonlinear eigenvalue problem: determine α and β subject to (1.11) such that the fourth-order ordinary differential equation (ODE)

$$(|f|^n f''')' = \alpha f + \beta \eta f'$$

has a solution $f \in C^4(0, \eta_0) \cap C^1[0, \eta_0]$ which is positive on $(0, \eta_0)$ and satisfies the boundary conditions

$$f(0) = f'(0) = f(\eta_0) = f'(\eta_0) = 0, |f|^n(\eta) f'''(\eta) \to 0 \quad \text{as } \eta \to \eta_0.$$

Here $\eta_0 > 0$ is arbitrary. A solution for $\eta_0 = 1$ gives a solution for arbitrary $\eta_0 > 0$ by scaling. Such self-similar solutions are called self-similar solutions of the second kind (the exception to this is the special case $n = 1$ in which (1.10) is a similarity solution of the first kind, with $\alpha = 1/3$, $\beta = 1/6$, because the first moment of h is conserved; again see [22]).

In Section 2 below we analyse this eigenvalue problem by transforming the (ODE) to a four-dimensional dynamical system and identifying the dipole type self-similar solution as a connection between two critical points, one of the two lying at infinity. For the analysis of the critical points at infinity we use a modification of the transformations used in [23]. The connection problem is solved by means of a detailed numerical investigation, which in particular makes possible the calculation of the anomalous exponents $\alpha(n)$. This is done in Section 3. One interesting feature is the appearance of a second family of self-similar solutions in the range $0 \leq n < 1/2$. These solutions have zero contact angle at both the fixed and the free boundary, and are specified by imposing optimal smoothness at the free boundary, characterised by the exponent $3/(n+1)$ (which is larger than the exponent 2). A similar family of solutions may be obtained for the Cauchy problem (cf. [20]). In the $n = 0$ limit case this corresponds to having h and its space derivatives upto order two vanishing at the free boundary, so that h is a solution of the obstacle problem for (1.4), the obstacle being $h \equiv 0$; see also the discussion at the end of Section 2 in [19]. Furthermore, we expect these solutions to exist in the whole of the range $-1 < n < 1/2$.

We anticipate that (1.10) also describes the asymptotic behaviour of (1.1), (1.7), (1.8) for $n_c < n \leq 0$ for some finite n_c, i.e. down to some (currently unknown) critical exponent. As in the case of the Cauchy problem ([20],[19]), we expect that for $n = n_c$

$$h \sim e^{-\alpha t} f(x/e^{-n_c \alpha t/4}) \text{ as } t \to \infty \text{ with } x = O(e^{-n_c \alpha t/4}) \tag{1.12}$$

and for $n < n_c$

$$h \sim (t_c - t)^{\alpha} f(x(t_c - t)^{\beta}) \text{ as } t \to t_c^- \text{ with } x = O((t_c - t)^{-\beta}), \tag{1.13}$$

this being a second kind solution to (1.1),(1.7), with $\alpha, \beta > 0$ satisfying $-n\alpha - 4\beta = 1$, which represents extinction at some finite time $t = t_c$ (by contrast, the corresponding solution to the Cauchy problem is of first kind, with $\alpha = \beta = -1/(n+4)$). We shall leave such issues for $n < 0$ largely as open problems, though we do give results for the limit $n \to -\infty$; in view of the status of (1.7) as a combination of the fixed boundary conditions of [24], for which finite time extinction occurs for $n < 0$, and of the moving boundary conditions of the Cauchy problem analysed in [20],[19], for which $n_c = -4$, we anticipate that the critical exponent n_c for (1.1),(1.7),(1.8) will satisfy $-4 < n_c < 0$, and that it is characterised by $\alpha/\beta \to 4/n$.

In Section 4 we address three asymptotic regimes, namely $n \to 1$, $n \to 2^-$ and $n \to -\infty$, using formal methods. Consideration of the first two arises from the rigorous results of [22] which cover the existence of (first kind) similarity solutions for $n = 1$ and $n = 2$; we show below how properties of these solutions determine the evolution to second kind behaviour for neighbouring values of n. The methods we adopt here are fairly widely applicable to problems involving quantities which are 'almost' conserved, enabling results from (special) first kind cases to be extended to yield insight into significantly more delicate second kind cases; existing results in this direction have usually involved perturbing off a closed form solution, using either the implicit function theorem (e.g [25, 26]) or renormalisation group ideas (e.g. [27]). Approaches of the type outlined in Sections 4.1 and 4.2 below seem more generally applicable in the study of second kind problems arising in a variety of contexts and look promising in terms of pointing the way to rigorous justification of the validity of the the second kind results, particularly in the PDE setting. The limit $n \to -\infty$ is also instructive, notably because it confirms and illustrates the finite time extinction behaviour conjectured above. We conclude in Section 5 with some brief discussion of other possible boundary conditions.

2 The dynamical system

In this section we identify the appropriate similarity solution in (1.10) as corresponding to a connection between two critical points of a dynamical system. We shall refer to this solution as the dipole, and to the corresponding connection as the dipole connection. The dipole is given by

$$h(x,t) = t^{-\alpha} f(x/t^{\beta}), \quad n\alpha + 4\beta = 1, \tag{2.1}$$

where the profile $f(\eta) \geq 0$ must solve

$$(f^n f''')' = \beta\eta f' + \alpha f, \quad 0 < \eta < \eta_0, \tag{2.2}$$

and satisfy the boundary conditions,

$$f(0) = f'(0) = f(\eta_0) = f'(\eta_0) = f(\eta_0)^n f'''(\eta_0) = 0. \tag{2.3}$$

Here η_0 is positive and may be used as scaling parameter. We restrict our attention to $0 < n < 2$.

In [23] we transformed (2.2) into a 4-dimensional quadratic system by setting

$$x = \frac{\eta f'}{f}; y = \frac{\eta^2 f''}{f}; z = \frac{\eta^3 f'''}{f}; u = \eta^4 f^{-n}; t = \log \eta, \tag{2.4}$$

where x and t are not to be confused with x and t in (1.1) and where for the time being we restrict attention to f and η positive. The system for x, y, z, u as functions of t reads

$$\begin{aligned} \dot{x} &= x(1-x) + y, \\ \dot{y} &= y(2-x) + z, \\ \dot{z} &= z(3-(n+1)x) + u(\alpha + \beta x), \\ \dot{u} &= u(4 - nx). \end{aligned} \tag{2.5}$$

This transformation maps positive solutions f of (2.2) to orbits of (2.5) in the half-space $H = \{u > 0\}$. To identify the dipole connection we need the local structure near the critical points, as determined in [23]: the critical points are

$$(0,0,0,0),\ (1,0,0,0),\ P_1 = (2,2,0,0),\ P_2 = (\frac{3}{n+1}, -\frac{-6+3n}{(n+1)^2}, \frac{(6n-3)(-2+n)}{(n+1)^3}, 0), \tag{2.6}$$

and

$$P_3 = (\frac{4}{n}, -\frac{4n-16}{n^2}, \frac{(-16+8n)(n-4)}{n^3}, \frac{(8n+32)(-2+n)(n-4)}{n^3(\alpha n + 4\beta)}). \tag{2.7}$$

Orbits coming out of these critical points into H correspond to solutions $f(\eta)$ defined on some interval $(0, \eta_0)$ with $0 < \eta_0 \leq \infty$. Near $\eta = 0$ they behave like $A\eta^b$ where b is the x-coordinate of the corresponding critical point. The constant $A > 0$ is arbitrary, except for P_3, for which it follows easily from the u-coordinate (in the range of α and n considered below there will be no such solutions). In [23] the number of degrees of freedom for these solutions with powerlike behaviour is determined from the linearisation of (2.5) around the corresponding critical point. Relevant for the analysis in this paper are the points

$$P_1 \ \text{ for } \ 0 < n < \frac{1}{2} \ \text{ and } \ P_2 \ \text{ for } \ \frac{1}{2} < n < 2, \tag{2.8}$$

corresponding to the exponents 2 and $\frac{3}{n+1}$, which are the exponents of the dipole for respectively $0 < n < \frac{1}{2}$ and $\frac{1}{2} < n < 2$, see [22]. In both cases the relevant critical point has a 2-dimensional unstable manifold, denoted by W^u, with tangent space spanned by two eigenvectors, as can easily be seen by counting the eigenvalues with positive real part of the linearisations

$$\begin{pmatrix} -3 & 1 & 0 & 0 \\ -2 & 0 & 1 & 0 \\ 0 & 0 & 1-2n & \alpha+2\beta \\ 0 & 0 & 0 & 4-2n \end{pmatrix} \quad \text{at } P_1 \text{ and } \quad \begin{pmatrix} \frac{n-5}{n+1} & 1 & 0 & 0 \\ \frac{-6+3n}{(n+1)^2} & \frac{2n-1}{n+1} & 1 & 0 \\ -\frac{(6n-3)(-2+n)}{(n+1)^2} & 0 & 0 & \frac{\alpha n+\alpha+3\beta}{n+1} \\ 0 & 0 & 0 & \frac{n+4}{n+1} \end{pmatrix} \quad \text{at } P_2.$$

In both cases there are two positive eigenvalues and one of the two eigenvectors has a non-zero u-component, because the right bottom entry of the matrix is positive and the other bottom entries are zero. Thus 'half' of W^u is contained in H. Also note that the matrices above and below may be simplified by putting $n\alpha + 4\beta = 1$.

In the light of the description above, we look for an orbit in $H \cap W^u$ with the appropriate large t behaviour. Let us first review the possiblities. We assume, as will be supported by the numerics, that orbits in $H \cap W^u$ have simple ω-limit sets, by which we mean singletons consisting of a single critical point, possibly at infinity.

Orbits in $H \cap W^u$ cannot lie in the stable manifolds of P_1 and P_2, because these stable manifolds are contained in $\partial H = \{u = 0\}$. This observation also applies to the other critical points with $u = 0$, provided $n < 2$. On the other hand, it is perfectly possible for an orbit in $H \cap W^u$ to connect to P_3, corresponding to solutions f having algebraic growth (exponent $\frac{4}{n}$). This point has linearisation, see [23],

$$\begin{pmatrix} \frac{n-8}{n} & 1 & 0 & 0 \\ \frac{4n-16}{n^2} & \frac{2n-4}{n} & 1 & 0 \\ -\frac{(-16+8n)(n-4)(\alpha n+\alpha+3\beta)}{n^2(\alpha n+4\beta)} & 0 & -\frac{n+4}{n} & \frac{\alpha n+4\beta}{n} \\ -\frac{(8n+32)(-2+n)(n-4)}{n^2(\alpha n+4\beta)} & 0 & 0 & 0 \end{pmatrix}. \tag{2.9}$$

For $n = 2$ the eigenvalues are $-3, -2, -1, 0$. The determinant of this matrix being $8(n+4)(n-2)(n-4)n^{-3}$, it follows that for n slightly smaller all eigenvalues are negative. Analysing the characteristic polynomial we find that there are no purely imaginary eigenvalues in the parameter range under consideration, which is $0 < n < 2$, $0 < n\alpha < 1$. Thus P_3 is an attractor and we can expect all bounded orbits to approach this point as $t \to \infty$, corresponding to solutions

$$f \sim \left(\frac{n^3}{8(n+4)(n-2)(n-4)}\right) \eta^{\frac{4}{n}} \text{ as } \eta \to \infty. \tag{2.10}$$

Next we consider the possibilities for orbits to go to infinity. In [23] this was done by means of the standard Poincaré transformation. Here we use a slightly modified form of this transformation, see also [28],[22], and set

$$x = \frac{X}{V}; y = \frac{Y}{V^2}; z = \frac{Z}{V^3}; u = \frac{U}{V^3}, \qquad X^2 + Y^2 + Z^2 + 2U = C, \tag{2.11}$$

where C is an arbitrary non-zero number. Note that we are restricted to $U, V > 0$. The standard Poincaré transformation would read

$$x = \frac{X}{V^2}; y = \frac{Y}{V^2}; z = \frac{Z}{V^2}; u = \frac{U}{V^2}, \qquad X^2 + Y^2 + Z^2 + U^2 + V^2 = C,$$

leading to five differential equations involving the derivatives of X, Y, Z, U and V from which these derivatives are calculated. Common factors are discarded by introducing a new independent variable which has no effect on the orbits of the system. One of the view modern texts on dynamical systems in which this transformation is discussed is [29]. Our modification consists of dropping V from the constraint, so that we may think of the new variables as living in a Poincaré cylinder rather than a sphere, and changing several exponents. The effect of changing the exponents is that we have a minimal number of critical points with a maximum of information from the linearisations of the differential equations around them. The choice here was found by trial and error and seems optimal, see also [22] where we use a slightly different modification to analyse a three-dimensional system for the construction of a dipole of the first kind for $n = 1$. The effect of taking a cylinder instead of a sphere (near the equator, i.e. near $V = 0$, a sphere looks like a cylinder) and replacing U^2 by $2U$ (we have $U > 0$ anyway) is that the new differential equations come out a little less complicated.

The new system reads

$$
\begin{aligned}
\dot{X} &= (-Y^2+(n-2)Z^2-\beta UZ+U(n-3))X^2-ZYX+2Y^3+(3U+3Z^2)Y\\
&\qquad -XU(1+Z\alpha)V,\\
\dot{Y} &= YX^3+ZX^2+(-2Y^2+((2n-1)Z^2-2\beta UZ+(2n-3)U)Y)X+3ZU+3Z^3\\
&\qquad -2YU(1+Z\alpha)V,\\
\dot{Z} &= ((-n+2)Z+U\beta)X^3+(((-2n+1)Z+2U\beta)Y^2-3YZ+3\beta U^2-3ZU)X\\
&\qquad -3YZ^2+U(3\alpha U+2\alpha Y^2+\alpha X^2-3Z)V,\\
\dot{U} &= (-n+3)UX^3+((-2n+3)UY^2-3YU+3UZ^2-3\beta U^2Z)X-3UYZ\\
&\qquad +U(X^2-3ZU\alpha+3Z^2+2Y^2)V,\\
\dot{V} &= (X^3+(Y^2-Y+(n+1)Z^2-\beta UZ+Un)X-YZ)V\\
&\qquad +(-ZU\alpha-3Z^2-X^2-4U-2Y^2)V^2.
\end{aligned}
\tag{2.12}
$$

Modulo the scaling $(a,b,c,d)\to(as,bs^2,cs^3,ds^3)$ the critical points at infinity ($V=0$) with $U\geq 0$ and $X\leq 0$ are

$$Q_1=(-1,0,0,0),\quad Q_2=(-1,\frac{1}{2},0,0),\quad Q_3=(-1,-\frac{1}{3}(n-2),-\frac{1}{9}(2n-1)(n-2),0), \tag{2.13}$$

$$Q_4=(-1,-\frac{1}{3}(n-3),-\frac{1}{9}(2n-3)(n-3),-\frac{1}{9\beta}(2n-3)(n-3))\ \text{for}\ 3/2\leq n\leq 3, \tag{2.14}$$

and $Q_5=(0,0,0,1)$. The point Q_1 has linearised matrix

$$
\begin{pmatrix}
0 & 0 & 0 & n-3 & 0\\
0 & -1 & 1 & 0 & 0\\
0 & 0 & -2+n & -\beta & 0\\
0 & 0 & 0 & n-3 & 0\\
0 & 0 & 0 & 0 & -1
\end{pmatrix}
\tag{2.15}
$$

and is an attractor (modulo the scaling), its eigenvalues being $-1,-1,n-2,n-3$ (ignoring in here and what follows the zero eigenvalue due to the scaling invariance).

None of the other points is an attractor. In the numerics below we will see that orbits in $W^u\cap H$ typically select one of the two attractors P_3 and Q_1. Standard continuity arguments imply that there must be an orbit in $W^u\cap H$ which is not in the domain of attraction of P_3 and Q_1. We refer to this orbit as the critical orbit, although we only have numerical evidence of its uniqueness. Tuning α we look for an α-value for which the critical orbit corresponds to a solution f satisfying (2.3). To this end, we will identify a critical point in whose 2-dimensional stable (fast stable if $n < \frac{1}{2}$) manifold the critical orbit must be contained for (2.3) to hold.

Generically we expect the critical orbit to connect to a critical point with a 3-dimensional stable manifold. As we explain next there are two such points and it depends an the value of α which of the two is selected by the critical orbit. The first possibility is $Q_5 = (0, 0, 0, 1)$, which has matrix

$$\begin{pmatrix} 0 & 3 & 0 & 0 & 0 \\ 0 & 0 & 3 & 0 & 0 \\ 3\,\beta & 0 & 0 & 0 & 3\,\alpha \\ 0 & 0 & 0 & 0 & 0 \\ 0 & 0 & 0 & 0 & 0 \end{pmatrix}. \tag{2.16}$$

and eigenvalues $0, 3\sqrt[3]{\beta}, \frac{3}{2}\sqrt[3]{\beta}(-1 - i\sqrt{3}), \frac{3}{2}\sqrt[3]{\beta}(-1 + i\sqrt{3})$. We note that this is the only point with $X = 0$ and this suggests that x may be bounded. Modifying (2.11) to

$$x = X; y = \frac{Y}{V}; z = \frac{Z}{V^2}; u = \frac{U}{V^3}, \qquad Y^2 + Z^2 + 2U = C, \tag{2.17}$$

we find (modulo scaling) only one critical point at $V = 0$ with $U \geq 0$, namely $\tilde{Q}_5 = (\frac{-\alpha}{\beta}, 0, 0, 1)$ which corresponds to Q_5 and has exactly the same eigenvalues. The point Q_5 has a 3-dimensional centre-stable manifold. We note that the zero eigenvalue is the only one with an eigenvector having non-zero V-component and that all orbits coming from $\{V > 0\}$ enter Q_5 along this vector. These observations are based on a WKBJ-analysis giving solutions of (2.2) with leading order term

$$f \sim A\eta^{-\frac{\alpha}{\beta}}, \tag{2.18}$$

and possible correction terms

$$\left(B_1 \cos\left(\frac{3\sqrt{3}\beta}{2}\left(\frac{\beta}{A^n}\right)^{\frac{1}{3}}\eta^{\frac{1}{3\beta}}\right), B_2 \sin\left(\frac{3\sqrt{3}\beta}{2}\left(\frac{\beta}{A^n}\right)^{\frac{1}{3}}\eta^{\frac{1}{3\beta}}\right)\right)\eta^{\frac{\alpha+2\beta-1}{3\beta}} \exp\left(-\frac{3\beta}{2}\left(\frac{\beta}{A^n}\right)^{\frac{1}{2}}\eta^{\frac{1}{3\beta}}\right). \tag{2.19}$$

We note that the non-zero eigenvalues are zeros of the same cubic appearing in the WKBJ-analysis. Numerically we find that the critical orbit connects to Q_5 for small α.

The other three points, Q_2, Q_3 and Q_4, are in direct correspondence to points discussed in [23], Sections 3.2, 3.3, 3.5. Their eigenvalues are, up to a positive multiple,

$$-1, 2, 2n - 1, 2n - 3 \ \text{ for } \ Q_2, \tag{2.20}$$

$$0, -(n+1), -3, -\frac{4n-5 \pm \sqrt{1+20n-8n^2}}{2} \quad \text{for} \quad Q_3, \tag{2.21}$$

$$3, -n, -\frac{4n-9 \pm \sqrt{-8n^2+36n-27}}{2} \quad \text{for} \quad Q_4. \tag{2.22}$$

For the last point the multiple changes sign as β changes sign.

For $\frac{1}{2} < n < \frac{3}{2}$ the point Q_2 has a 2-dimensional stable manifold W^s containing solutions with the required interface behaviour: zero contact angle and flux, zero flux following from

$$\frac{z(t)}{u(t)} = \frac{1}{\eta} f(\eta)^{n-1} f'''(\eta) \to \beta, \tag{2.23}$$

and quadratic behaviour near η_0. Here (2.23) follows from the matrix corresponding to Q_2,

$$\begin{bmatrix} \frac{1}{2} & \frac{1}{2} & \frac{1}{2} & -\frac{3}{2}+n & 0 \\ 1 & 1 & 1 & \frac{3}{2}-n & 0 \\ 0 & 0 & -\frac{3}{4}+\frac{3}{2}n & -\frac{3}{2}\beta & 0 \\ 0 & 0 & 0 & -\frac{9}{4}+\frac{3}{2}n & 0 \\ 0 & 0 & 0 & 0 & -\frac{3}{4} \end{bmatrix}$$

which (consistent with (2.20) above) has eigenvalues $-\frac{3}{4}$, $\frac{3}{2}$, $\frac{3}{4}(2n-1)$ and $\frac{3}{4}(2n-3)$, the latter being the negative eigenvalue closest to zero, with eigenvector

$$\left(\frac{2}{3}\left(\frac{\beta}{2n-5}+1\right), \frac{2}{3}\left(\frac{2\beta}{2n-5}-1\right), \beta, 1, 0\right)$$

being responsible for (2.23). We note that this is independent of the sign of β, so that in this range fronts may move in either direction. Thus in this range, to construct the dipole, we need to tune α so as to make the critical orbit connect to Q_2. For $n > \frac{3}{2}$ the stable manifold is contained in $V = 0$ and may be ignored (it will appear below that in this range we have to connect the critical orbit to Q_4). For $0 < n < \frac{1}{2}$, however, it is 3-dimensional, but only the orbits coming in along eigenvectors corresponding to the two most negative eigenvalues have (2.23). Thus we must tune α to make the critical orbit connect to Q_2 along this fast stable manifold. Solutions connecting to Q_2 along the generic eigenvector (eigenvalue $2n-1$, both directions allowed) do not have zero flux.

The stable manifold of Q_3 contains solutions $f(\eta)$ which go to zero as $\eta \to \eta_0$ as a power-function with exponent $\frac{3}{n+1}$. For $\frac{1}{2} < n < 2$ its dimension is 3, and the critical orbit goes into

Q_3 for α too large. For $0 < n < \frac{1}{2}$ however, the dimension is 2, and Q_3 takes over from Q_2. In this range we can also tune α to make the critical orbit connect to Q_3. Solutions thus obtained have non-zero flux and gain, rather than conserve, mass at the interface, but do represent the smoothest non-negative solutions for this range of n.

Finally there is Q_4, which for $\frac{3}{2} < n < 3$ takes over the role of Q_2, having W^s with dimension 2 and containing the zero flux, zero contact angle solutions (exponent $\frac{3}{n}$ near η_0), so that for $\frac{3}{2} < n < 2$ we tune α to connect the critical orbit to Q_4. For $n < \frac{3}{2}$ this point has $U < 0$ and is not relevant here, while the point $-Q_4$ has a 3-dimensional stable manifold contained in $V = 0$ and is also irrelevant here.

3 Numerical construction of the trajectories

3.1 Preliminaries

In this section we outline the numerical approach used to construct the trajectories (outlined in the previous section) between local equilibrium points and those at infinity. The approach is based on a shooting method program which follows trajectories emanating from the linearized unstable manifold of the relevant local equilibrium point. These trajectories may either escape to infinity or approach some other local equilibrium point.

The program is based around NAG routine D02PAF and solves equations (2.5) using a Runge-Kutta-Merson technique. For the work featured here, we always shoot from a two-dimensional unstable manifold and the initial values for x, y, z and u come from choosing points on a closed curve $(x, y, z, u) = \mathbf{\Gamma}(\theta)$, traced out by the (single-valued) function $\mathbf{\Gamma}(\theta)$ defined by

$$\mathbf{\Gamma} = \mathbf{P_c} + (\mathbf{a}\cos\theta + \mathbf{b}\sin\theta)\,, \tag{3.1}$$

where $\mathbf{a}$ and $\mathbf{b}$ represent (sufficiently small) eigenvectors corresponding to the unstable eigenvalues of the relevant critical point $\mathbf{P_c}$ (namely P_1 or P_2) and $\theta \in [0, 2\pi)$, restricting attention to $u > 0$; in practice we take $|\mathbf{a}| = |\mathbf{b}| = d$ with $d = 0.1$.

Solutions of (2.5), which, in terms of (2.11) converge to one of the points Q_1, Q_2, Q_3, Q_4, escape to infinity in finite t, having $y \sim ax^2$, where a is the Y-coordinate of Q_i in (2.13)-(2.14). These solutions correspond (see [23]) to solutions $f(\eta)$ with local interface behaviour

$$f \sim A(\eta_0 - \eta)^{\frac{1}{1-a}} \text{ as } \eta \to \eta_0^- . \tag{3.2}$$

For clarity we include Table 1 which lists this correspondence and all possible behaviours, including convergence to Q_5 or P_3. The dimension of the stable manifold as n varies for each equilibrium point is also included in Table 1. We note that Q_5 corresponds to solutions satisfying $x \to -\alpha/\beta$ as the solution escapes to infinity as $t \to \infty$, whence (2.18). As explained in Section 2 we look for connections to Q_1-Q_5 and in particular, tuning α and θ, to Q_i's with $\dim(W^s) = 2$.

			$\dim(W^S)$		
Equilibrium point	f-behaviour	$y \sim ax^2$	$n < \frac{1}{2}$	$\frac{1}{2} < n < \frac{3}{2}$	$\frac{3}{2} < n < 2$
Q_1	$f \sim (\eta_0 - \eta)^1$	$a = 0$	4		
Q_2	$f \sim (\eta_0 - \eta)^2$	$a = \frac{1}{2}$	3	2	0
Q_3	$f \sim (\eta_0 - \eta)^{\frac{3}{n+1}}$	$a = \frac{2-n}{3}$	2	3	3
Q_4	$f \sim (\eta_0 - \eta)^{\frac{3}{n}}$	$a = \frac{3-n}{3}$	1	2	2
Q_5	$f \sim \eta^{-\frac{\alpha}{\beta}}$	-	3		
P_3	$f \sim \eta^{\frac{4}{n}}$	-	4 $(0 < n\alpha < 1)$		

Table 1: Possible f-behaviours and dimension of the stable manifold of the corresponding critical point.

We recognise escape to infinity in finite time with $y \sim ax^2$ by projecting the trajectories onto the $(\log |x|, \log |y|)$ plane, noting that points where a trajectory crosses an axis in the (x, y) plane correspond to asymptotes in the log plot. As trajectories escape to infinity in the log plot we therefore expect them to have gradient 2 (corresponding to reaching Q_2, Q_3 or Q_4), gradient less then 2 (corresponding to reaching Q_1), or $x \to 4/n$ or $x \to -\alpha/\beta$ (corresponding to P_3 and Q_5, but these are better seen in a plot of x versus t). Additionally, if we extrapolate a line with slope 2 we find an intercept of $\log(a)$ (see Figure 2).

To find the critical pair of values that corresponds to the dipole solution we perform numerical simulations varying α and θ. For fixed α we first determine the critical θ-value for which the solution is non-generic (i.e. not in the domain of attraction of P_3 or Q_1). This θ-value is denoted by $\theta_c(\alpha)$. We then vary α to obtain a pair $(\alpha_c, \theta_c(\alpha_c))$ for which the solution connects to a critical point (Q_2 or Q_4) with $\dim(W^s)$=2. This α_c is the anomalous dipole exponent. For $n < 1/2$ the situation is slightly different; see Section 2 and Section 3.4 below.

3.2 Behaviour for $1/2 < n < 3/2$

In this range of n we look for the orbit connecting the two-dimensional unstable manifold of P_2 to the two-dimensional stable manifold of Q_2 (Table 1 shows this point to relate to the required quadratic behaviour for f local to the interface). The behaviour of orbits coming out of P_2 in this regime, described in terms of the (α, θ) parameter plane, is shown in the schematic in Figure 1. The numbers which are not contained in parentheses represent the exponent in the second column of Table 1. Numbers contained in braces denote the dimension of stable manifolds.

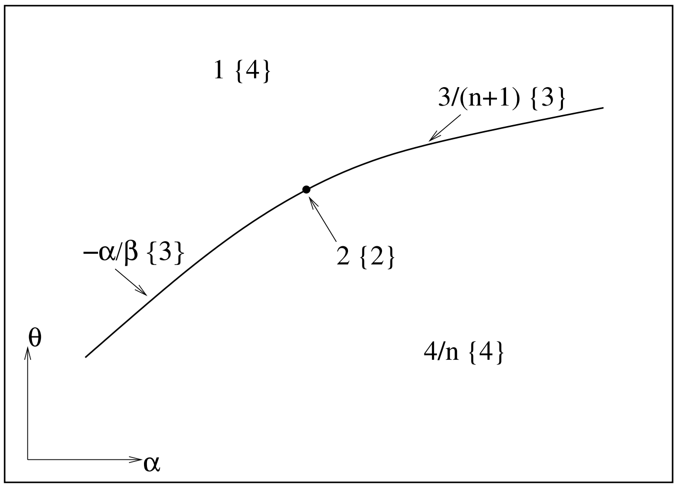

Figure 1: Schematic of the behaviour of trajectories in the (α, θ) plane for $1/2 < n < 3/2$.

Figure 2(a) shows the critical $(\alpha_c,\, \theta_c(\alpha_c))$ solution for $n = 1.2$. In this case $\alpha_c \approx 0.30317$. From the additional straight line superimposed on the graph we see that the gradient of the solution in the far-field is 2 and that the intercept of the straight line is given by $\log(1/2)$, as desired. For the non-generic solution with $\alpha > \alpha_c$ we pick up the behaviour governed by Q_3 as shown in Figure 2(b) (cf. Figure 1). For $(\alpha, \theta_c(\alpha))$ with $\alpha > \alpha_c$, by inspection of the x-t graph we see that the solutions have $x \to -\alpha/\beta$ as $t \to \infty$ (as far as numerical accuracy will allow), corresponding to Q_5. We note that it is a consequence of unavoidable numerical inaccuracies that the solution eventually escapes to one of the generic behaviours (see Figure 2(c)). It is thus difficult to recognise this solution in terms of the $\log x$, $\log y$ plot, as the required solution has x and y converging to a specific point - numerical errors take the solution away from this point and the fact that the trajectory moves slowly in its neighbourhood is not apparent from a plot involving x and y but not t.

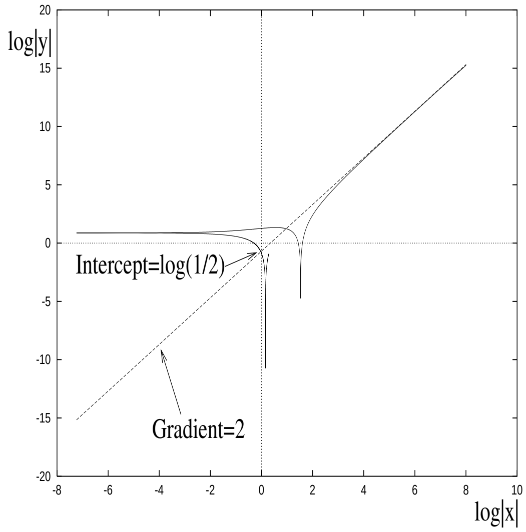

(a) $(\alpha_c, \theta_c(\alpha_c))$

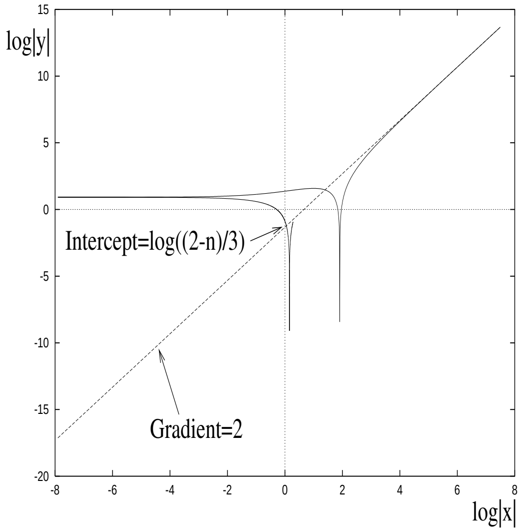

(b) $(\alpha > \alpha_c, \theta_c(\alpha))$

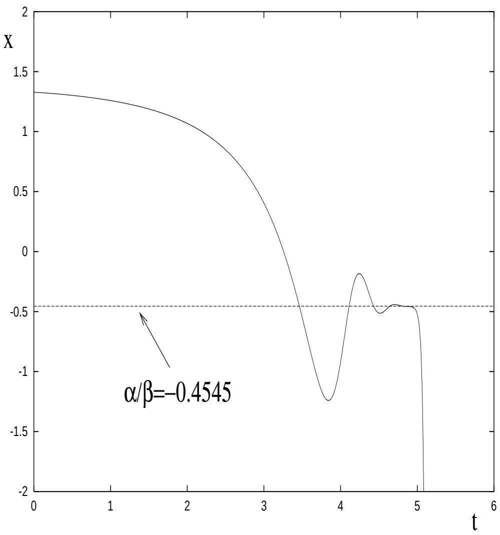

(c) $(\alpha < \alpha_c, \theta_c(\alpha))$

Figure 2: Critical trajectories that reach infinity for $n = 1.2$.

Figure 3 shows the dipole connection for $n = 1$ found numerically and this is consistent with the analysis in [22] (for $n = 1$ the first moment of h is conserved which fixes $\alpha = 1/3$), helping to validate the numerical approach.

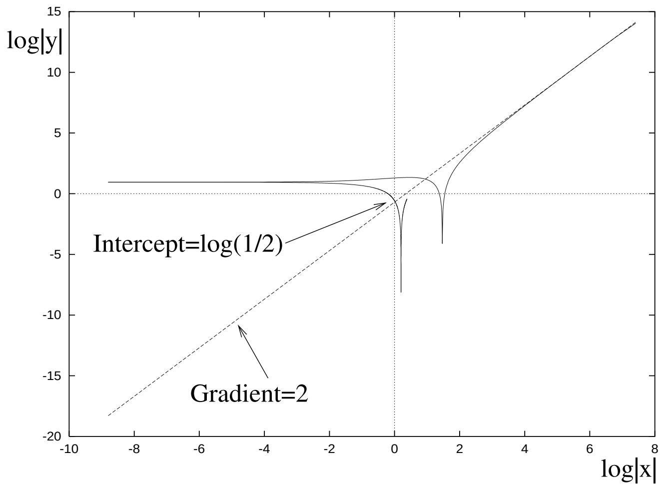

Figure 3: Graph of the $(\alpha_c, \theta_c(\alpha_c))$ solution for $n = 1$ with $\alpha_c = 1.0/3.0$ and $\theta_c(\alpha_c) \approx 1.5676027$.

3.3 Behaviour for $3/2 < n < 2$

For $3/2 < n < 2$ we retain most of the structure that exists for $1/2 < n < 3/2$, the only change being that the stable manifold of Q_2 becomes one-dimensional and that of Q_4 two-dimensional (cf. Section 2). Q_4 takes over from Q_2 and is the relevant equilibrium point for the dipole solution in this range of n. The (α, θ) parameter plane illustrating the structure of the phase space is shown in Figure 4, where we employ the same notation as discussed in Figure 1.

Figure 5(a) shows the critical trajectory representing the dipole solution for $n = 1.8$. We see that the superimposed straight line has intercept log $(3 - n)/3$ and gradient 2, as desired. For completeness we also include Figures 5(b) and (c) to illustrate the behaviour of non-generic solutions on each side of the dipole solution.

3.4 Behaviour for $0 < n < 1/2$

In this regime, the behaviour is more complex in that we now have two possible critical connections. We can find either a connection between the two-dimensional unstable manifold of P_1 and the two-dimensional stable manifold of Q_3, or we may also connect to the fast two-dimensional stable manifold of Q_2. The situation is illustrated in Figure 6.

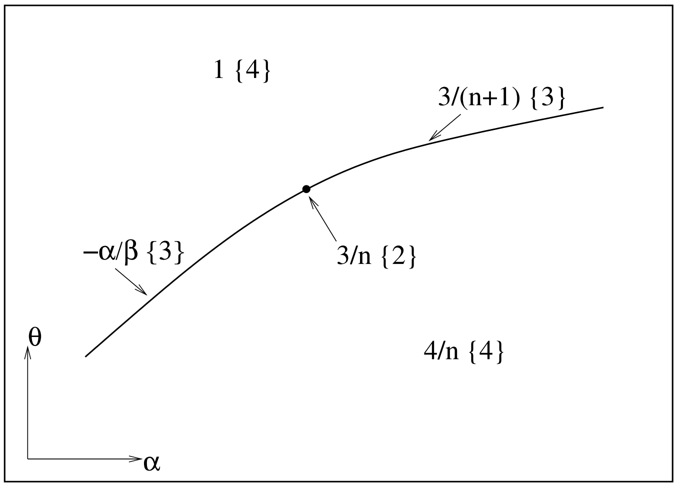

Figure 4: Schematic of the behaviour of trajectories in the (α, θ) plane for $3/2 < n < 2$.

We comment at this point that such zero flux solutions with quadratic interface behaviour are found by studying graphs of z against t for the non-generic solutions. The zero flux solution has $z \to 0$ as $t \to \infty$ in correspondence with Q_2 while all other non-generic solutions have z escaping to infinity.

The solutions with interface behaviour $f \sim (\eta_0 - \eta)^{3/(n+1)}$ as $\eta \to \eta_0$ are particularly sensitive to numerical errors and it is difficult to locate these solutions by numerical study of (2.5). This problem persists for all $n < 1/2$ and so we use a different numerical methodology in this case. We solve (2.2) directly by shooting from $\eta = 0$ with initial conditions adapted from [24], namely

$$f \sim \eta^2 + B\eta^{3-2n} \text{ as } \eta \to 0, \tag{3.3}$$

(with B being determined as part of the solution) and find the value of η_0 such that $f(\eta_0) = f'(\eta_0) = 0$ for fixed α. Varying α then allows us to construct graphs of η_0 against α for various n, see Figure 7. The critical value of α that we seek is the minimum α value for each curve. Here the transition from f having a minimum to f having a maximum in η_0 occurs. Thus we also find that $f''(\eta_0) = 0$, consistent only with Q_3. It is noteworthy that the branches of solutions can be continued (and now correspond to solutions with sign changes), but fold back. It is this borderline behaviour which causes the above noted numerical difficulties; as is to be expected, they become more severe as $n \to 1/2$. We determine the sign change branches

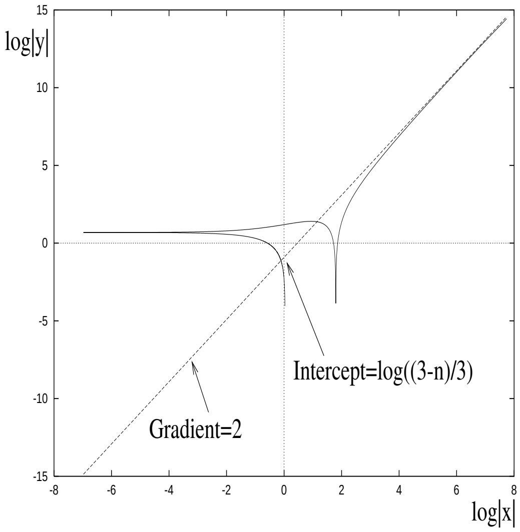

(a) $(\alpha_c, \theta_c(\alpha_c))$

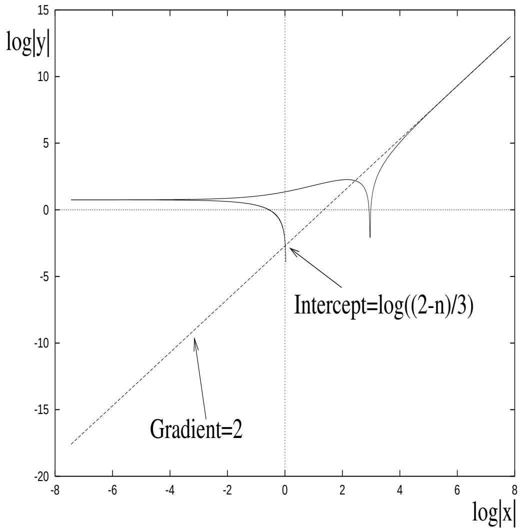

(b) $(\alpha, \theta_c(\alpha))$, $\alpha > \alpha_c$

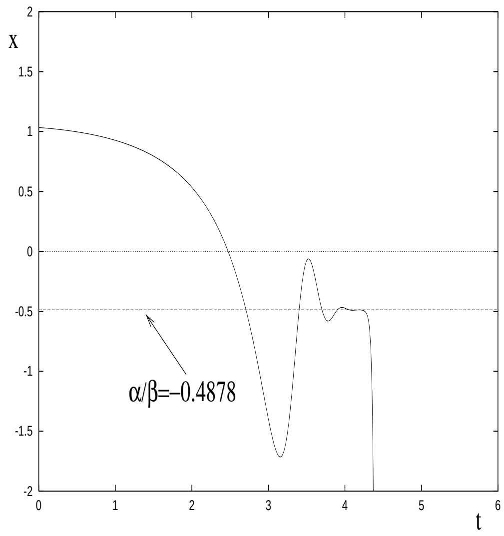

(c) $(\alpha, \theta_c(\alpha))$, $\alpha < \alpha_c$

Figure 5: Critical trajectories that reach infinity for $n = 1.8$.

numerically only for $n = 0$, this being discussed below. Note that the form of the dynamical system (2.5) makes it inconvenient to find trajectories representing solutions with sign changes. Moreover, numerous different branches of sign change solutions can be specified, depending on how the local behaviour at a zero of h is prescribed; those given below for $n = 0$ are analytic

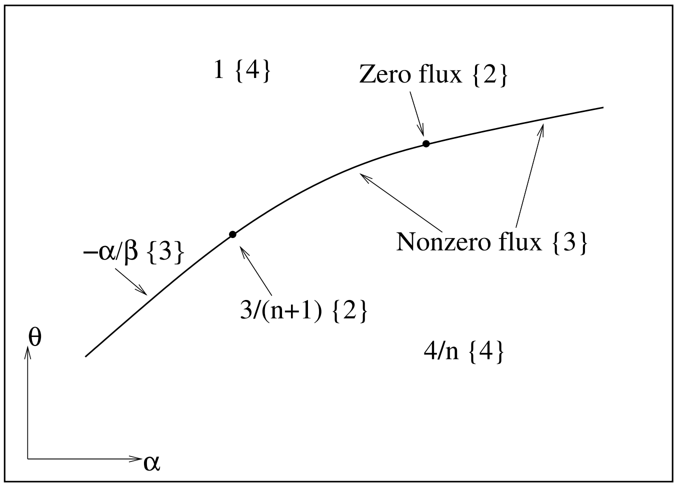

Figure 6: Schematic of the behaviour of trajectories in the (α, θ) plane for $0 < n < 1/2$.

at a zero.

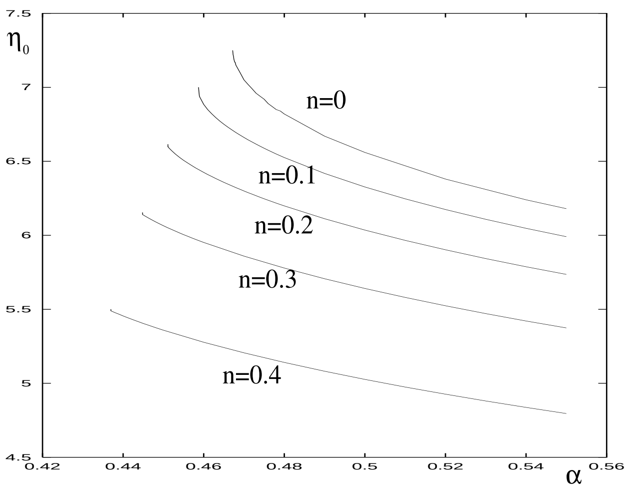

Figure 7: Graph of η_0 against α for various $n \in [0, 1/2)$.

For $n = 0$ we may easily construct additional branches of solutions featuring sign changes and having zero contact angle at their free boundary. It is the linearity of (2.2) that allows us to continue the solutions through zero without difficulty and find further values of η_0 for which zero contact angle conditions hold at the interface. We proceed by fixing α and then separating the initial condition (3.3) into two parts, denoting the solution of (2.2) with $f = \eta^2 + o(\eta^3)$ as

f_1 and the solution with $f \sim \eta^3$ as f_2. Values of η_0 at which the Wronskian, $W(f_1(\eta_0), f_2(\eta_0))$, becomes zero correspond to solutions of $f(\eta_0) = f_1(\eta_0) + Bf_2(\eta_0) = 0$, with zero contact angle at the interface. The first zero of W corresponds to the positive solution discussed above and B is specified from the requirement that $f_1(\eta_0) + Bf_2(\eta_0) = 0$. By counting zeros and varying α we then build up branches of solutions displayed as η_0 against α in Figure 8. Each fold corresponds to an increase in the number of sign changes. We use numbers in braces to denote the number of sign changes in the solution, so that $\{0\}$ denotes the branch of non-negative solutions.

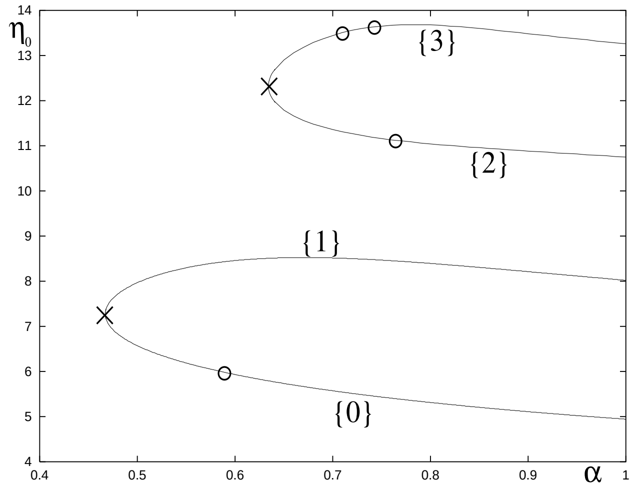

Figure 8: Graph of η_0 against α for $n = 0$ illustrating branches of zero contact angle sign change solutions. Crosses indicate solutions with $f''(\eta_0) = 0$ and circles label solutions with $f'''(\eta_0) = 0$. Note that, somewhat surprisingly, there appear to be no zero flux solutions that contain a single interior zero, but there are two with three interior sign changes; moreover no $f''(\eta_0) = 0$ solution with a single interior zero manifests itself.

3.5 The overall picture

By combining the approaches from the previous sub-sections we may construct the graph of α_c against n, as shown in Figure 9. The $3/(n+1)$ branch merges with $\alpha_c(n)$ as $n \to 1/2^-$; the numerics become increasingly delicate as n approaches $1/2$ and 2, resulting in the gaps in the curves. It is noteworthy that the asymptotics about $n = 2$ indicate a rather rapid change in α in that neighbourhood.

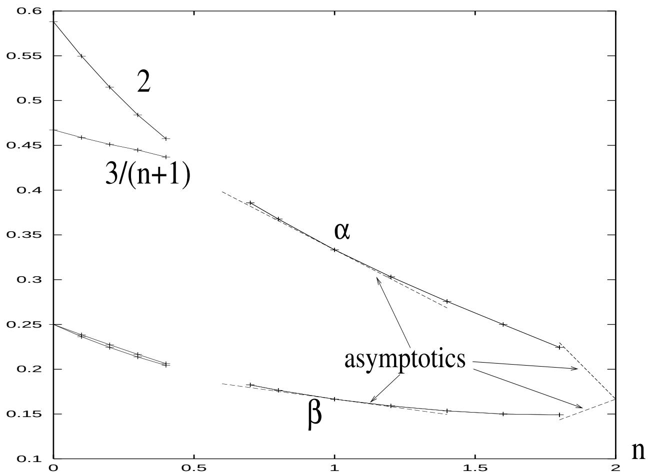

Figure 9: Graph of exponents of the exceptional connections against n. The (dashed) straight lines show the asymptotic results (4.12), (4.26) derived below.

4 Asymptotic results

In this section we investigate the behaviour of the anomalous exponent and its corresponding dipole solution in the limit cases $n \to 1$, $n \uparrow 2$ and $n \downarrow -\infty$. This will be done by means of formal asymptotics for the full PDE.

4.1 $n \to 1$

In this limit we can exploit the result from [22] that for $n = 1$ the asymptotic solution is of the first kind (due to conservation of the first moment), with

$$h \sim t^{-\frac{1}{3}} f(x/t^{\frac{1}{6}}) \text{ as } t \to \infty. \tag{4.1}$$

We write $n = 1 + \varepsilon$ with $|\varepsilon| \ll 1$ and analyse the limit $\varepsilon \to 0$ on the timescale $\tau = |\varepsilon| \ln t = O(1)$ in which deviations from (4.1) are significant. It is easy to show that, for $-1 < \varepsilon < 1/2$,

$$\frac{d}{dt}\int_0^s xh dx = \frac{1}{2}\varepsilon(1+\varepsilon)\int_0^s h^{\varepsilon-1}\left(\frac{\partial h}{\partial x}\right)^3 dx,$$

this being for small ϵ an 'almost conserved' quantity of the type mentioned in the introduction, so writing

$$h = t^{-\frac{1}{3}} F(\eta, \tau), \qquad s = t^{\frac{1}{6}} \sigma(\tau), \qquad \eta = x/t^{\frac{1}{6}}, \tag{4.2}$$

yields

$$\frac{d}{d\tau} \int_0^\sigma \eta F \, d\eta = \frac{1}{2}(1+\varepsilon)\mathrm{sgn}(\varepsilon) e^{-\frac{1}{3}\mathrm{sgn}(\varepsilon)\tau} \int_0^\sigma F^{\varepsilon-1} \left(\frac{\partial F}{\partial \eta}\right)^3 d\eta. \tag{4.3}$$

We now apply formal asymptotic methods and expand $F \sim F_0(\eta,\tau) + \epsilon F_1(\eta,\tau)$ as $\varepsilon \to 0$. It follows from (1.1) and (4.2) that

$$\frac{1}{6}\left(2F_0 + \eta \frac{\partial F_0}{\partial \eta}\right) = e^{-\frac{1}{3}\mathrm{sgn}(\varepsilon)\tau} \frac{\partial}{\partial \eta}\left(F_0 \frac{\partial^3 F_0}{\partial \eta^3}\right), \tag{4.4}$$

with the most general solution to (4.4) of the required form being

$$F_0 = e^{\frac{1}{3}\mathrm{sgn}(\varepsilon)\tau} \phi^4(\tau) f(\eta/\phi(\tau)), \tag{4.5}$$

where $\phi(\tau)$ is a (currently arbitrary) scaling function and $f(\xi)$ represents the solution (4.1) for $n = 1$, so that $f(\xi)$ is determined by (here we use ξ rather than η to denote the independent variable to avoid confusion with η in (4.5))

$$\frac{1}{6}\xi^2 f = \xi f \frac{d^3 f}{d\xi^3} - f\frac{d^2 f}{d\xi^2} + \frac{1}{2}\left(\frac{df}{d\xi}\right)^2, \quad f(0) = f(\xi_0) = \frac{df}{d\xi}(\xi_0) = 0, \tag{4.6}$$

(both the other boundary conditions

$$\frac{df}{d\xi}(0) = f(\xi_0)\frac{d^3 f}{d\xi^3}(\xi_0) = 0$$

are then automatically satisfied simultaneously, corresponding in the second kind framework to $\alpha = 1/3$ being the eigenvalue for $n = 1$). If $f(\xi)$ satisfies (4.6) then so does $\xi_0^4 f(\xi/\xi_0)$; ξ_0 in the $n = 1$ problem is fixed by conservation of first moment

$$\int_0^{\xi_0} \xi f(\xi) d\xi = \int_0^a x h_0(x) dx, \tag{4.7}$$

but in the current context it is more convenient to specify f uniquely by imposing $\xi_0 = 1$, which henceforth we do; it then follows that $\sigma(\tau) \sim \phi(\tau)$ as $\epsilon \to 0$. Note that the presence of the arbitrary function $\phi(\tau)$ in (4.5) is a consequence of the solution to (4.6) being required to satisfy the side condition (4.7), so that (4.6) of necessity possesses a one-parameter family of solutions. Such considerations apply much more generally in second kind scenarios in which a special case is of first kind, as does the procedure which we now outline for determining $\phi(\tau)$

from the almost conserved quantity. Thus the expression (4.3) provides a solvability condition which determines the scaling factor $\phi(\tau)$, whereby

$$\int_0^1 \xi f d\xi \,\frac{d}{d\tau}\left(e^{\frac{1}{3}\mathrm{sgn}(\varepsilon)\tau}\phi^6(\tau)\right) = \frac{1}{2}\mathrm{sgn}(\varepsilon)\int_0^1 f^{-1}\left(\frac{df}{d\xi}\right)^3 d\xi e^{\frac{1}{3}\mathrm{sgn}(\varepsilon)\tau}\phi^6(\tau). \tag{4.8}$$

In view of (4.6) we have

$$\int_0^1 f^{-1}\left(\frac{df}{d\xi}\right)^3 d\xi = 2\int_0^1 \xi\left(\frac{d^2 f}{d\xi^2}\right)^2 d\xi - \frac{2}{3}\int_0^1 \xi f d\xi,$$

so, defining the positive constants μ and ν by

$$\mu = \int_0^1 \xi\left(\frac{d^2 f}{d\xi^2}\right)^2 d\xi, \qquad \nu = \int_0^1 \xi f d\xi, \tag{4.9}$$

equation (4.8) yields

$$\phi(\tau) = \phi_0 \exp\left(\frac{1}{6}\left(\frac{\mu}{\nu} - \frac{2}{3}\right)\mathrm{sgn}(\varepsilon)\tau\right), \tag{4.10}$$

for some constant ϕ_0 which is determined by matching into the timescale $t = O(1)$ in which the leading order problem is simply that for $n = 1$; ϕ_0 thus depends only on the first moment of the initial data, having the value ξ_0 determined by (4.6)-(4.7). For $\tau = O(1)$ we thus have

$$\int_0^s xh dx \sim \nu\phi_0^6 \exp\left(\left(\frac{\mu}{\nu} - \frac{1}{3}\right)\mathrm{sgn}(\varepsilon)\tau\right) \quad \text{as } \varepsilon \to 0. \tag{4.11}$$

Hence, using $\exp(\mathrm{sgn}(\epsilon)\tau) = t^{\epsilon}$, we have that (4.5) takes the conjectured form (1.10) with

$$\alpha \sim \frac{1}{3} - \left(\frac{2\mu}{3\nu} - \frac{1}{9}\right)\varepsilon, \qquad \beta \sim \frac{1}{6} + \left(\frac{\mu}{6\nu} - \frac{1}{9}\right)\varepsilon \qquad \text{as } \varepsilon \to 0, \tag{4.12}$$

consistent with (1.11). We find by computing $f(\xi)$ numerically that

$$\mu \approx 1.5998 \times 10^{-4}, \qquad \nu \approx 3.9023 \times 10^{-4} \tag{4.13}$$

so β is decreasing near $n = 1$ and $3\mu > \nu$, as might be expected.

4.2 $n \to 2^-$

The analysis here is similar, relying on the first kind result for $n = 2$ that

$$h \sim t^{-\frac{1}{6}} f(x/t^{\frac{1}{6}}) \text{ as } t \to \infty,$$

the borderline case $n = 2$ lying in the mass preserving regime (see [22]). We write $n = 2 - \delta$ with $0 < \delta \ll 1$ and $\tau = \delta \ln t$. The analysis of this case relies on the local result from [22] that for $0 < \delta < 3/2$

$$h \sim \left(\frac{(3-\delta)^3}{3(3-2\delta)\delta} J(t) x^3 \right)^{\frac{1}{3-\delta}} \quad \text{as } x \to 0^+, \tag{4.14}$$

where $J(t)$ is defined in (1.9), so that

$$\frac{d}{dt} \int_0^s h dx = -J(t); \tag{4.15}$$

because (4.14) implies that $J = O(\delta)$ as $\delta \to 0$, (4.15) represents another almost conserved quantity and considerations very similar to those in Section 4.1 again apply. In this case we need to write

$$h = t^{-\frac{1}{6}} F(\eta, \tau), \qquad s = t^{\frac{1}{6}} \sigma(\tau), \qquad \eta = x/t^{\frac{1}{6}}, \qquad J = \delta K(\tau)/t, \tag{4.16}$$

giving to leading order as $\delta \to 0^+$ that

$$\frac{1}{6} \left(F_0 + \eta \frac{\partial F_0}{\partial \eta} \right) = e^{\frac{1}{6}\tau} \frac{\partial}{\partial \eta} \left(F_0^2 \frac{\partial^3 F_0}{\partial \eta^3} \right),$$

from which it follows that

$$F_0 = e^{-\frac{1}{12}\tau} \phi^2(\tau) f(\eta/\phi(\tau)), \tag{4.17}$$

where $f(\xi)$ gives the (mass preserving) similarity solution for $n = 2$, which we again specify by choosing $\xi_0 = 1$ rather than by imposing the conservation law, which in this case takes the form

$$\int_0^{\xi_0} f(\xi) d\xi = \int_0^a h_0(x) dx.$$

Here $f(\xi)$ is given by

$$\frac{1}{6}\xi = f \frac{d^3 f}{d\xi^3}, \quad f(0) = f(\xi_0) = \frac{df}{d\xi}(\xi_0) = 0,$$

so that if $f(\xi)$ is a solution then so is $\xi_0^2 f(\xi/\xi_0)$, the existence of such a one-paramter family again underpinning the appearance of the arbitrary function $\phi(\tau)$ in (4.17). Setting $\xi_0 = 1$, so that $\sigma(\tau) \sim \phi(\tau)$ as $\delta \to 0$, it follows that

$$-\frac{1}{12}(1 - \xi^2) = f \frac{d^2 f}{d\xi^2} - \frac{1}{2} \left(\frac{df}{d\xi} \right)^2,$$

so that

$$\frac{df}{d\xi} = \frac{1}{\sqrt{6}} \text{ at } \xi = 0. \tag{4.18}$$

We now need the result that the local expression (4.14) also provides the leading order solution as $\delta \to 0^+$ in the (exponentially small) inner region $\zeta = O(1)$ with $\zeta < 0$, where $\zeta = \delta \ln \eta$, in which $G(\zeta, \tau) = F(\eta, \tau)/\eta$ is given to leading order by

$$G_0(\zeta, \tau) = (3K_0)^{\frac{1}{3}} e^{\frac{1}{3}\zeta - \frac{1}{18}\tau}, \tag{4.19}$$

writing $K \sim K_0(\tau)$ as $\delta \to 0^+$. The quantity $F_0(\eta, \tau)$, introduced above, represents the leading order solution in the outer region $\eta = O(1)$ and matching with (4.19) as $\zeta \to 0$ thus requires that

$$F_0 \sim (3K_0)^{\frac{1}{3}} e^{-\frac{\tau}{18}} \eta \text{ as } \eta \to 0^+; \tag{4.20}$$

it then follows from (4.17)-(4.18) that

$$e^{-\frac{1}{12}\tau} \phi^3 = 6^{\frac{3}{2}} 3 K_0, \tag{4.21}$$

this being the first of the two relations between $\phi(\tau)$ and $K_0(\tau)$ that we require. The second comes from (4.15)-(4.17), which yield

$$\frac{d}{d\tau}\left(\kappa e^{-\frac{1}{12}\tau} \phi^3\right) = -K_0, \tag{4.22}$$

where

$$\kappa = \int_0^1 f \, d\xi. \tag{4.23}$$

Finally, (4.21)-(4.22) imply

$$\phi = \phi_0 \exp\left(\frac{1}{36}\left(1 - \left(\frac{2}{3}\right)^{\frac{1}{2}} \frac{1}{3\kappa}\right)\tau\right), \qquad K_0 = \frac{\phi_0^3}{6^{\frac{3}{2}} 3} \exp\left(-\frac{1}{6^{\frac{3}{2}} 3\kappa}\tau\right), \tag{4.24}$$

where $\phi_0 = \phi(0)$ is determined by the mass of the initial data, the leading order problem for $t = O(1)$ being that with $n = 2$. It follows from (4.24) that for $\tau = O(1)$

$$\int_0^s h \, dx \sim \kappa \phi_0^3 \exp\left(-\frac{1}{6^{\frac{3}{2}} 3\kappa}\tau\right) \tag{4.25}$$

(which, as is to be expected, decays with τ) and that, since $\exp(\tau) = t^\delta$,

$$\alpha \sim \frac{1}{6} + \frac{1}{36}\left(1 + \left(\frac{2}{3}\right)^{\frac{1}{2}} \frac{2}{3\kappa}\right)\delta, \qquad \beta \sim \frac{1}{6} + \frac{1}{36}\left(1 - \left(\frac{2}{3}\right)^{\frac{1}{2}} \frac{1}{3\kappa}\right)\delta \qquad \text{as } \delta \to 0^+, \tag{4.26}$$

consistent with (1.11). Numerically we find that $\kappa \approx 5.2641 \times 10^{-2}$. Additionally α decreases monotonically with n and $3\kappa < (2/3)^{\frac{1}{2}}$, $3\mu < 2\nu$, with β decreasing from $1/4$ at $n = 0$ through $1/6$ at $n = 1$ before subsequently rising again to reach $1/6$ at $n = 2$ (see Figure 10).

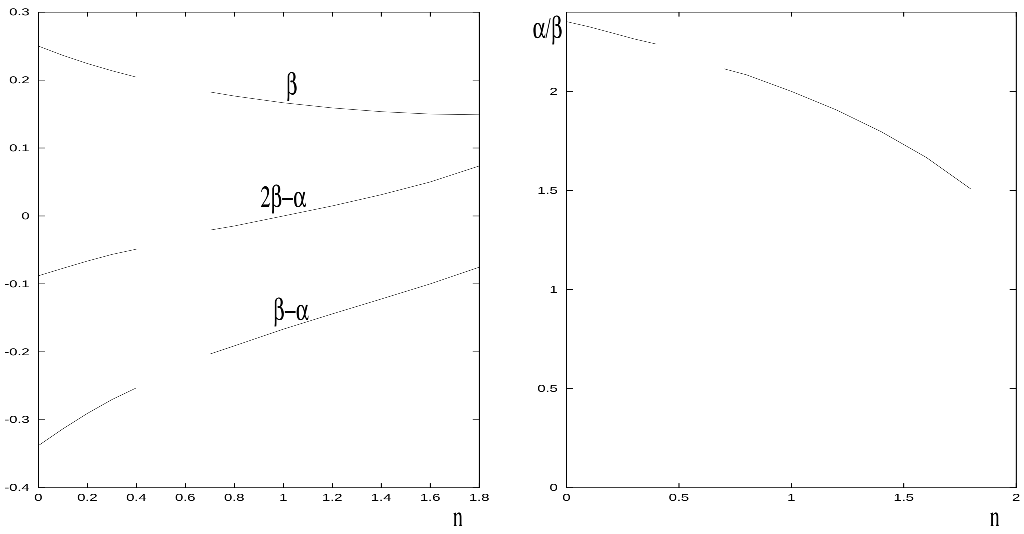

(a) (b)

Figure 10: Graphs comparing the values of (a) β, $2\beta - \alpha$ (first moment), $\beta - \alpha$ (mass) against n and (b) α/β against n.

We note that the timescale $\tau = O(1)$ corresponds to exponentially large t, the rate of loss of mass being extremely slow. This analysis therefore clarifies the apparently abrupt transition noted in [22] between mass loss for $n < 2$ and mass conservation for $n \geq 2$.

4.3 $n \to -\infty$

Letting $n \to -\infty$ we have in particular $n < n_c$ so that (1.13) applies. We note that n_c may be characterised by the fact that the rescaled ODE for f, namely

$$(f^n f''')' = \eta f' + \lambda f, \qquad \lambda = \frac{\alpha}{\beta}, \tag{4.27}$$

has a positive solution with $f(0) = f'(0) = f(1) = f'(1) = \lim_{n \uparrow 1} f^n(1) f'''(1) = 0$ precisely for $\lambda = -4/n$.

The analysis partly follows that of [24]. We write $n = -1/\nu$ and take the limit $\nu \to 0^+$; we scale such that $h_0(x_0) = \max h_0 = 1$ and assume h_0 to be monotonic either side of $x = x_0$.

The initial evolution occurs over the exponentially short timescales $t^\nu = O(1) < 1$; we have

$$h \sim h_I x^2 / q_-^2 \qquad 0 < x < q_-(t),$$

$$h \sim h_0(x) \qquad q_-(t) < x < q_+(t),$$
$$h \sim h_I(s_0 - x)^2/(s_0 - q_+)^2 \quad q_+(t) < x < s_0(t),$$

with $h_I(t) = t^\nu$ and where $q_- < x_0$ and $q_+ > x_0$ are defined by $h_0(q_\pm) = h_I$; the leading order interface position $s_0(t)$ is then determined by conservation of mass, giving (recalling $s(0) = a$)

$$\frac{1}{3}h_I(s_0 - q_+) = \int_{q_+}^{a} h_0(x)dx.$$

When h_I reaches one, each of q_- and q_+ coincide with x_0; a slow phase of evolution then occurs (cf.[24]), of which we omit details, leading on to the final regime of exponentially short timescales $(t_c - t)^\nu = O(1) < 1$ which are of most interest to us here since they govern the extinction behaviour, whereby $h \equiv 0$ for $t \geq t_c$. Defining $h_m(t;\nu)$ to be the maximum of $h(x,t)$, located at $x = q(t;\nu)$ say, the evolution proceeds as follows.

Writing $h_m \sim h_m^0(t)$, $q \sim q_0(t)$ as $\nu \to 0$, we have the outer solutions

$$\begin{aligned} &h \sim h_m^0 x^2/q_0^2 && 0 < x < q_0(t) \\ &h \sim h_m^0(s_0 - x)^2/(s_0 - q_0)^2 && q_0(t) < x < s_0(t). \end{aligned} \tag{4.28}$$

The inner scalings

$$x = q(t;\nu) + \nu z, \qquad h = h_m(1 - \nu\rho) \tag{4.29}$$

yield

$$\frac{dh_m}{dt} + h_m \frac{dq_0}{dt}\frac{\partial \rho_0}{\partial z} \sim \nu^{-3} h_m^{(\nu-1)/\nu} \frac{\partial}{\partial z}\left(e^{\rho_0}\frac{\partial^3 \rho_0}{\partial z^3}\right) \tag{4.30}$$

so that

$$\begin{aligned} &e^{\rho_0}\frac{\partial^3 \rho_0}{\partial z^3} = -dz + b\rho_0 + c, \\ &\rho_0 \sim 2(-z)/q_0 \text{ as } z \to -\infty, \\ &\rho_0 = \frac{\partial \rho_0}{\partial z} = 0 \text{ at } z = 0, \\ &\rho_0 \sim 2z/(s_0 - q_0) \text{ as } z \to +\infty, \end{aligned} \tag{4.31}$$

where the quantities b, c and d are independent of ν, with

$$-\nu^3 h_m^{(1-\nu)/\nu}\frac{dh_m}{dt} \sim d, \qquad \nu^3 h_m^{1/\nu}\frac{dq_0}{dt} \sim b, \tag{4.32}$$

and c arises on integrating (4.30). The constraints in (4.31) correspond to six boundary conditions, so are in principle sufficient to determine $d(q_0, s_0)$, $b(q_0, s_0)$ and $c(q_0, s_0)$, as well as

$\rho_0(z; q_0, s_0)$. Two leading order ODE's for the three unknowns h_m, q_0 and s_0 are then provided by (4.32); the third follows from conservation of mass, which implies that

$$\frac{d}{dt}\int_q^s h\,dx = \left(-\frac{dq}{dt}h + h^{-1/\nu}\frac{\partial^3 h}{\partial x^3}\right)\Bigg|_{x=q^+}$$

and hence from the second of (4.28) that

$$\frac{d}{dt}\left(\frac{1}{3}h_m^0(s_0 - q_0)\right) = -h_m^0\frac{dq_0}{dt}. \tag{4.33}$$

Further information can be deduced from the scaling properties of (4.31). Writing $q_0(t) = \phi(t)s_0(t)$, where $0 < \phi < 1$, together with $z = s_0 Z$, $d = D/s_0^4$, $b = B/s_0^3$ and $c = C/s_0^3$, yields

$$\begin{aligned}
&e^{\rho_0}\frac{\partial^3\rho_0}{\partial Z^3} = -D(\phi)Z + B(\phi)\rho_0 + C(\phi),\\
&\rho_0 \sim 2(-Z)/\phi \text{ as } Z \to -\infty,\\
&\rho_0 = \frac{\partial\rho_0}{\partial Z} = 0 \text{ at } Z = 0,\\
&\rho_0 \sim 2Z/(1-\phi) \text{ as } Z \to +\infty,
\end{aligned} \tag{4.34}$$

which determines $D(\phi)$, $B(\phi)$, $C(\phi)$ and $\rho_0(Z;\phi)$; the boundary value problem (4.34) is the key ingredient in governing the evolution. The system (4.32)-(4.33) can now be reduced at leading order to

$$\begin{aligned}
&h_m^0 = (t_c - t)^\nu,\\
&\frac{1}{q_0}\frac{dq_0}{dt} = \frac{\lambda(\phi)}{h_m^0}\frac{dh_m^0}{dt},\\
&\frac{d}{dt}\left(\frac{1-\phi}{3\phi}h_m^0 q_0\right) = -h_m^0\frac{dq_0}{dt},
\end{aligned} \tag{4.35}$$

where we have written $\lambda(\phi) = B(\phi)/\phi D(\phi)$ (the appearance of the small parameter ν in the leading order expression h_m is acceptable because the behaviour we are outlining takes place on the timescale $T = O(1)$, where $T = -\nu\ln(t_c - t)$, implying $h_m^0(T) = \exp(-T)$; however, for brevity we shall retain $t_c - t$ throughout this description). As $t \to t_c^-$ we have $\phi(t) \to \phi_c$, a constant, corresponding to the required self-similar behaviour, with, using (4.35),

$$\begin{aligned}
&q_0 \sim k_c(t_c - t)^{-\nu\lambda(\phi_c)},\\
&\frac{1-\phi_c}{3\phi_c}(1 - \lambda(\phi_c)) = \lambda(\phi_c),
\end{aligned}$$

where the constant k_c depends on the initial data. Hence ϕ_c is determined by

$$\lambda(\phi_c) = (1-\phi_c)/(1+2\phi_c) \tag{4.36}$$

where $\lambda(\phi)$ is (in principle) known from (4.34). Unfortunately, it does not seem possible to obtain ϕ_c explicitly, but it follows from (4.34) that D is even and B is odd about $\phi - 1/2$ and we anticipate that $D > 0$ and that $B > 0$ for $\phi < 1/2$; this implies that $0 < \phi_c < 1/2$. Since we have $\lambda(\phi_c) < 1$, we can conclude that we have finite time extinction, with the mass tending to zero as $t \to t_c^-$. Finally, using $\alpha - 4\nu\beta = \nu$ we obtain

$$\alpha \sim \nu + 4\nu^2\lambda(\phi_c), \qquad \beta \sim \nu\lambda(\phi_c) \qquad \text{as } \nu \to 0^+. \tag{4.37}$$

5 Discussion

We have mainly been concerned in this paper with the one-dimensional thin film equation (1.1) for zero contact angle conditions, imposing zero flux at the free boundary (1.7). Numerous generalisations are also amenable to the approaches we have adopted; the one to which we restrict our discussion here replaces zero contact angle conditions in (1.1) by zero pressure ones (such a possibility was already noted in [22]), giving

$$\begin{aligned} &h = \frac{\partial^2 h}{\partial x^2} = 0 && \text{at } x = 0 \text{ and } x = s(t) \quad \text{(zero pressure)}, \\ &\lim_{x\uparrow s(t)} h^n \frac{\partial^3 h}{\partial x^3} = 0 && \text{at } x = s(t) \quad \text{(zero flux)}, \end{aligned} \tag{5.1}$$

The conditions at $x = 0$ in (5.1) are admissible if $n < 1$ and the conditions at $x = s(t)$ if $n < 2$; these ranges can be extended if the second derivative boundary conditions are replaced by the constraints that the x^2 and $(s - x)^2$ terms be absent from the relevant local expansions - at $x = 0$ the first two terms are then of the form x and x^{3-n} (so the constraint is admissible for $n < 2$ but has unbounded second derivative if $n > 1$) and at $x = s$ they are $(s - x)$ and $(s - x)^{4-n}$ (admissible for $n < 3$ but unbounded second derivative if $n > 2$).

Our main observation concerning (5.1) is that first kind behaviour now occurs for $n = 0$ rather that $n = 1$ (as noted in [30], these are the values of n for which (1.1) admits conservation laws other than conservation of mass). Indeed, for $n = 0$ we have

$$\frac{d}{dt}\int_0^{s(t)} xh(x,t)dx = -\left[x\frac{\partial^3 h}{\partial x^3} - \frac{\partial^2 h}{\partial x^2}\right]_0^{s(t)}, \tag{5.2}$$

so the first moment is conserved when (5.1) holds, giving

$$h(x,t) \sim t^{-\frac{1}{2}} f(x/t^{\frac{1}{4}}) \text{ as } t \to \infty \tag{5.3}$$

as the relevant asymptotic behaviour (in fact, (5.3) is simply the x-derivative of the zero contact angle source solution for $n = 0$ given in [20]); for other n a new second kind formulation is required and a new critical exponent n_c will arise.

Sign change scenarios provide other avenues for further investigation, leading to discrete spectra of second kind exponents (cf. [4]). Figure 8 illustrates a particular case with $n = 0$; for this exponent, a possible limit behaviour as the number of sign changes tends to infinity can be deduced from

$$\frac{d}{dt}\int_0^\infty x^2 h dx = -\left[x^2\frac{\partial^3 h}{\partial x^3} - 2x\frac{\partial^2 h}{\partial x^2} + 2\frac{\partial h}{\partial x}\right]_0^\infty, \tag{5.4}$$

which implies that the second moment is conserved (so that $\alpha = 3/4$) for solutions to (1.1) with $n = 0$ which decay in an oscillatory fashion as $x \to \infty$ and satisfy zero contact angle conditions at $x = 0$. Figure 8 indeed indicates that $\alpha = 3/4$ is a plausible limit for both crosses and circles as the number of sign changes tends to infinity; however, the third moment of h is also conserved, as is $\int_0^\infty \Phi(x,t)hdx$ for any Φ with $\Phi_t = \Phi_{xxxx}$, $\Phi(0,t) = \Phi_x(0,t) = 0$ and with Φ not blowing up exponentially fast as $x \to +\infty$ (there being an infinite number of suitable polynomial solutions for Φ), so there is a family of other (more non-generic) limit solutions, further illustrating the complexity of such formulations.

The above examples illustrate the variety of distinct prescriptions which are available for (1.1); this is to be contrasted with the much more widely studied second-order case (1.2), for which the only choice of boundary conditions relevant in the current context is

$$\begin{aligned} &\text{at } x = 0 && h = 0, \\ &\text{at } x = s(t) && h = h^n\frac{\partial h}{\partial x} = 0. \end{aligned} \tag{5.5}$$

The higher-order case (1.1) not suprisingly admits an infinite number of analogs of (5.5), of which (1.7) and (5.1) are arguably the most significant mathematically, at least for $n > 1/2$.

Acknowledgements

JH and JRK gratefully acknowledge the support of the NWO/British Council and MB that of the TMR network Nonlinear Parabolic Partial Differential Equations: Methods and Applications (ERBFMRXCT980201). JRK is also grateful for the support of the Leverhulme Trust. Finally, we thank F. Bernis for stimulating discussions.

A1 Appendix 1: The 'drainage' boundary conditions

The conditions we impose at $x = 0$ are relevant when fluid is able to drain over an edge, but (because such configurations lead to somewhat delicate issues regarding contact line motion around an edge) we prefer to motivate them here by taking $\{y = 0, x < 0\}$ to be a thin porous substrate at the bottom of which a large negative pressure (suction) is imposed (other formulations involving highly porous layers lead to equivalent results); $\{y = 0, x > 0\}$ is an impermeable substrate with $y = h(x,t)$ being the free surface of the fluid. The simplest appropriate model is then

$$\frac{\partial h}{\partial t} = -\frac{\partial}{\partial x}\left(h^n \frac{\partial^3 h}{\partial x^3}\right) - \frac{1}{\epsilon} H(h) H(-x), \tag{A1.1}$$

where H is the Heaviside function (i.e. the characteristic function of $(0,\infty)$) We assume (A1.1) to imply that

$$[h]_-^+ = [\frac{\partial h}{\partial x}]_-^+ = [\frac{\partial^2 h}{\partial x^2}]_-^+ = [h^n \frac{\partial^3 h}{\partial x^3}]_-^+ = 0 \quad \text{at} \quad x = 0, \tag{A1.2}$$

and impose zero contact angle (finite contact angle would also be allowed in the derivations below) and zero flux free boundary conditions

$$h = \frac{\partial h}{\partial x} = h^n \frac{\partial^3 h}{\partial x^3} = 0 \quad \text{at} \quad x = -S(t), \tag{A1.3}$$

in which $x = -S(t) < 0$ is the left-hand interface; we are not concerned here with the behaviour at the right-hand interface $x = s(t) > 0$.

We shall give brief details of the limit $\epsilon \to 0^+$, thereby deriving our 'drainage' boundary conditions and clarifying the borderline status of $n = 2$; the outer formulations in question are those which are selected from (A1.1)-(A1.3) through that limiting process. Restricting ourselves to the moving contact line regime $n < 3$, there are three subcases to address; the local behaviour as $x \to (-S(t))^+$ takes the from

$$h \sim b(t)(x + S)^2 \quad (n < 1), \tag{A1.4}$$

$$h \sim (\frac{(n+1)^3}{8\epsilon(3-n)(n-1)})^{\frac{1}{n+1}} (x + S)^{\frac{4}{n+1}} \quad (1 < n < 3), \tag{A1.5}$$

where $b(t)$ is determined as part of the solution.

For $n < \frac{1}{2}$ we have inner scalings

$$x = \epsilon\hat{x},\ S = \epsilon\hat{S},\ h = \epsilon^2\hat{h},\ h \sim \hat{h}_0(\hat{x}, t) + \epsilon^{1-2n}\hat{h}_1(\hat{x}, t), \tag{A1.6}$$

the last of which already highlights the exceptional status of $n = \frac{1}{2}$. We thus obtain for $\hat{x} > -J$ that

$$\hat{h}_0 = B(t)(\hat{x} + J)^2, \quad B^n(\hat{x} + J)^{2n}\frac{\partial^3 \hat{h}_1}{\partial \hat{x}^3} = -J - \hat{x}H(-\hat{x}), \tag{A1.7}$$

and that $\hat{S}_0 = J$. Here $B(t)$ and $J(t)$ are determined from the outer solution via (A1.8) below; we have $b \sim B$ in (A1.4). Matching outwards, we thus have for $x = O(1)$ with $x > 0$ that the leading order outer solution satisfies

$$h \sim Bx^2 - \frac{1}{2(3-2n)(1-n)(1-2n)}\frac{J}{B^n}x^{3-2n} \quad \text{as} \quad x \to 0^+, \tag{A1.8}$$

which gives the local behaviour corresponding to the conditions (1.5) at $x = 0$ (cf. [22]).

For $\frac{1}{2} < n < 2$, we instead have

$$x = \epsilon\hat{x},\ S = \epsilon\hat{S},\ h = \epsilon^{\frac{3}{n+1}}\hat{h}, \tag{A1.9}$$

with the leading order inner problem (for $\hat{x} > -J$) being that

$$\hat{h}_0^n\frac{\partial^3 \hat{h}_0}{\partial \hat{x}^3} = -J - \hat{x}H(-\hat{x}), \quad \hat{S}_0 = J, \tag{A1.10}$$

with

$$\hat{h}_0 = \frac{\partial \hat{h}_0}{\partial \hat{x}} = 0 \quad \text{at} \quad x = -J(t), \tag{A1.11}$$

$$[\hat{h}_0]_-^+ = [\frac{\partial \hat{h}_0}{\partial \hat{x}}]_-^+ = [\frac{\partial^2 \hat{h}_0}{\partial \hat{x}^2}]_-^+ = 0 \quad \text{at} \quad x = 0, \tag{A1.12}$$

$$\hat{h}_0 \sim (\frac{(n+1)^3 J}{3(2-n)(1-2n)})^{\frac{1}{n+1}}\hat{x}^{\frac{3}{n+1}} \quad \text{as} \quad \hat{x} \to +\infty. \tag{A1.13}$$

An eigenmode count shows that (A1.13) corresponds to a single boundary condition, as required. The outer solution thus satisfies

$$h \sim (\frac{(n+1)^3 J}{3(2-n)(1-2n)})^{\frac{1}{n+1}}x^{\frac{3}{n+1}} \quad \text{as} \quad x \to 0^+, \tag{A1.14}$$

which holds in this regime when (1.5) holds, with $J(t)$ again being determined as part of the outer solution.

Finally, for $2 < n < 3$ the consequences of the analysis are significantly different, the outer solution which is selected having $J = 0$. The appropriate inner scalings are

$$x = \epsilon^{\frac{1}{3-n}}\hat{x},\ S = \epsilon^{\frac{1}{3-n}}\hat{S},\ h = \epsilon^{\frac{1}{3-n}}\hat{h}, \tag{A1.15}$$

with the leading order inner problem (for $\hat{x} > -\hat{S}_0$) being

$$\hat{h}_0^n \frac{\partial^3 \hat{h}_0}{\partial \hat{x}^3} = -\hat{S}_0 - \hat{x} H(-\hat{x}), \tag{A1.16}$$

with

$$\hat{h}_0 = \frac{\partial \hat{h}_0}{\partial \hat{x}} = 0 \quad \text{at} \quad x = -\hat{S}_0(t), \tag{A1.17}$$

$$[\hat{h}_0]_-^+ = [\frac{\partial \hat{h}_0}{\partial \hat{x}}]_-^+ = [\frac{\partial^2 \hat{h}_0}{\partial \hat{x}^2}]_-^+ = 0 \quad \text{at} \quad x = 0, \tag{A1.18}$$

$$\hat{h}_0 \sim A(t)\hat{x} \quad \text{as} \quad \hat{x} \to +\infty. \tag{A1.19}$$

The differences from the previous regime are instructive: with $A(t)$ given by the outer solution, the constraint (A1.19) amounts to two boundary conditions, so that (A1.16)-(A1.19) determine both $\hat{S}_0$ and $\hat{h}_0$, with scaling arguments implying that $\hat{S}_0 A^{-(n+1)/(3-n)}$ is a constant; more importantly, it follows that the flux from the outer region to the inner is $O(\epsilon^{(n-2)/(3-n)})$ (and, moreover, can be shown to decay as $t^{-(n+5)(n-2)/(n+4)(3-n)}$ as $t \to \infty$ for a mass preserving zero contact angle outer solution), confirming that the selected outer solution is that with no flux through $x = 0$, i.e. that satisfying (1.6) there. The transition to finite flux as n drops below two is clear from the exponent of ϵ just noted.

The key points arising from the above asymptotic analysis can be summarised as follows. (i) From amongst the members of the infinite family of possible solutions, characterised in [22] by their behaviour at $x = 0$, the limit $\epsilon \to 0^+$ in (A1.1)-(A1.3) above selects the smoothest one, namely the zero contact angle branch (1.5) for $n < 2$ and the no flux branch (1.6) for $2 < n < 3$. (ii) The boundary conditions with which we are concerned thus arise naturally in this physical context, as well as in a number of others; moreover, from the mathematical point of view the semi-infinite domain problems with which we are concerned can be regarded as representing the next step up from the Cauchy problem, which has been the subject of a great deal of analysis.

A2 Appendix 2: The doubly nonlinear equation

A2.1 Introduction

Our purpose here is two-fold: firstly to indicate briefly that our results generalise rather directly to the doubly nonlinear equation

$$\frac{\partial h}{\partial t} = -\frac{\partial}{\partial x}\left(h^n\left|\frac{\partial^3 h}{\partial x^3}\right|^{m-1}\frac{\partial^3 h}{\partial x^3}\right), \quad m > 1, \tag{A2.1}$$

and, secondly, to use (A2.1) to provide additional physical motivation for studying equation (1.1) for general n, the points to emphasise being that the discussion of the latter is significantly more transparent and that, in the current context, no additional phenomena arise for (A2.1). We thus believe it to be sensible to limit our detailed analysis to (1.1): it is the subject of a great deal of current mathematical interest and is extremely challenging in its own right; moreover, the results provide a great deal of insight into more general (and yet more difficult) formulations such as (A2.1).

A2.2 Local behaviour

It is clear from (A2.1) that the local balance

$$h \sim B(t)x^2 - \frac{m^3}{2(3m-2n)(m-n)(m-2n)}\frac{|J(t)|^{\frac{1}{m}-1}J(t)}{B(t)^{\frac{n}{m}}}x^{\frac{3m-2n}{m}} \quad \text{as} \quad x \to 0^+, \tag{A2.2}$$

in which J can have either sign, is self-consistent if $n < m/2$, so that $n = m/2$ generalises to (A2.1) the critical exponent $n = 1/2$ of (1.1); moreover,

$$h \sim \left(\left(\frac{(n+m)^3}{3m(2m-n)(2n-m)}\right)^m J(t)\right)^{\frac{1}{n+m}} x^{\frac{3m}{n+m}} \quad \text{as} \quad x \to 0^+ \tag{A2.3}$$

provides the relevant local behaviour for $m/2 < n < 2m$, with

$$J(t) \equiv -h^n\left|\frac{\partial^3 h}{\partial x^3}\right|^{m-1}\frac{\partial^3 h}{\partial x^3}\Bigg|_{x=0}$$

then required to be positive. Thus $n = 2m$ is the critical exponent for (A2.1) which generalises $n = 2$ for (1.1); no drainage is possible for $n > 2m$, $J \leq 0$ then being required.

A2 Physical motivation

Here we follow [31] in considering the two-dimensional spreading of a slender droplet of power-law fluid, governed at leading order by the lubrication theory balance

$$0=-\frac{\partial p}{\partial x}+\frac{\partial}{\partial y}(\mu_0\left|\frac{\partial u}{\partial y}\right|^{q-1}\frac{\partial u}{\partial y}),\quad 0=-\frac{\partial p}{\partial y},\quad \frac{\partial u}{\partial x}+\frac{\partial v}{\partial y}=0 \tag{A2.4}$$

with

$$\sigma_{xy}=0,\quad p=-\gamma\frac{\partial^2 h}{\partial x^2},\quad \frac{\partial h}{\partial t}=v-u\frac{\partial h}{\partial x}\quad \text{at}\quad y=h, \tag{A2.5}$$

where (u,v) is the velocity, q is a positive constant, μ_0 and γ are the viscosity and surface tension coefficients and the shear stress is given by

$$\sigma_{xy}=\mu_0\left|\frac{\partial u}{\partial y}\right|^{q-1}\frac{\partial u}{\partial y};$$

we generalise previous discussions by considering a power-law slip law along the substrate of the form

$$u=\lambda|\sigma_{xy}|^{\beta-1}\sigma_{xy},\quad v=0\quad \text{at}\quad y=0,$$

where β is a positive constant. We have

$$\frac{\partial h}{\partial t}+\frac{\partial}{\partial x}(\int_0^h u dy)=0,\quad \frac{\partial u}{\partial y}=-\frac{1}{\mu_0^{\frac{1}{q}}}(h-y)^{\frac{1}{q}}\left|\frac{\partial p}{\partial x}\right|^{\frac{1}{q}-1}\frac{\partial p}{\partial x},\quad p=-\gamma\frac{\partial^2 h}{\partial x^2},$$

so, writing $u=U$ at $y=0$,

$$\frac{\partial h}{\partial t}=\frac{q}{(2q+1)\mu_0^{\frac{1}{q}}}\frac{\partial}{\partial x}(h^{\frac{2q+1}{q}}\left|\frac{\partial p}{\partial x}\right|^{\frac{1}{q}-1}\frac{\partial p}{\partial x})-\frac{\partial}{\partial x}(hU); \tag{A2.6}$$

we note in (A2.6) that the first term on the right-hand side is independent of β and the second of q. If the q-term in (A2.6) dominates the final one, we obtain (to within a scaling) (A2.1) with

$$n=\frac{2q+1}{q},\quad m=\frac{1}{q}\quad (n=m+2), \tag{A2.7}$$

while if the converse is true (slip dominant, this typically being the case in practice when h is close to zero) we have, since

$$\sigma_{xy}=-h\frac{\partial p}{\partial x}\quad \text{on}\quad y=0,$$

equation (A2.1) with

$$n=\beta+1,\quad m=\beta\quad (n=m+1). \tag{A2.8}$$

In addition, the evolution under capillarity of a slender droplet of power-law fluid in a Hele-Shaw cell is shown in [31] to be governed by (A2.1) with

$$n = 1, \quad m = \frac{1}{q}. \tag{A2.9}$$

Shear thinning fluids have $0 < q < 1$ and shear thickening ones $q > 1$; hence for sufficiently shear thinning fluids ($0 < q < 1/2$), (A2.7) lies in the range $m/2 < n < 2m$; superlinear slip laws ($\beta > 1$ in (A2.8)) also have $m/2 < n < 2m$; for $1/2 < q < 2$ (Newtonian and moderately shear thinning and thickening fluids) Hele-Shaw flows have $m/2 < n < 2m$, while sufficiently shear thinning ones ($0 < q < 1/2$) have $n < m/2$. Hence the various qualitative ranges described in the main body of this paper are readily encompassed by models arising in applications; other related formulations with arbitrary n also arise in practice, including degenerate mobility versions of the Cahn-Hilliard equation (e.g. [32]).

References

[1] L.M. Hocking. Sliding and spreading of thin two-dimensional drops. *Q. J. Mech. Appl. Math.*, 34:37–54, 1981.

[2] R. Almgren, A. Bertozzi, and M.P. Brenner. Stable and unstable singularities in the unforced Hele-Shaw cell. *Phys. Fluids*, 8:1356–1370, 1996.

[3] H.P. Greenspan. On the motion of a small viscous droplet that wets a surface. *J. Fluid Mech.*, 84:125–143, 1978.

[4] J. Hulshof, J. R. King, and M. Bowen. Intermediate asymptotics of the porous medium equation with sign changes. To appear in Adv. Diff. Equ., `http://www.cs.vu.nl/~jhulshof/PAPERS/37.ps`.

[5] D. G. Aronson. The porous medium equation. *Some Problems in Nonlinear Diffusion, eds. A. Fasano & M. Primicerio, Lecture Notes in Math., CIME Foundation Series, Springer Verlag*, 1224, 1986.

[6] M. Muskat. *The Flows of Homogeneous Fluids through Porous Media.* McGraw-Hill, New York, 1937.

[7] S. Kamin. Asymptotic behaviour of solutions of the porous medium equation with changing sign. *SIAM Jour. Math. Anal.*, 22:34–45, 1991.

[8] E. Beretta, M. Bertsch, and R. Dal Passo. Nonnegative solutions of a fourth-order nonlinear degenerate parabolic equation. *Arch. Rat. Mech. Anal.*, 129:175–200, 1995.

[9] A.L. Bertozzi. Symmetric singularity formation in lubrication-type equations for interface motion. *SIAM J. Appl. Math.*, 56:681–714, 1996.

[10] F. Bernis. Viscous flows, fourth order nonlinear degenerate parabolic equations and singular elliptic problems. *Pitman Research Notes in Mathematics*, 323:40–56, 1995.

[11] A.L. Bertozzi, M.P. Brenner, T.F. Dupont, and L.P. Kadanoff. Singularities and similarities in interface flows. *Trends and Perspectives in Applied Mathematics, ed. L. Sirovich, Springer-Verlag*, 100:155–208, 1994.

[12] T. G. Myers. Thin films with high surface tension. *SIAM Rev.*, 40:441–462, 1998.

[13] J. Hulshof. Some aspects of the thin film equation. *Proceedings of 3ECM2000, Barcelona.* To appear, `http://www.cs.vu.nl/~jhulshof/PAPERS/48.pdf`.

[14] F. Bernis and J. B. McLeod. Similarity solutions of a higher order nonlinear diffusion equation. *Nonlin. Anal.*, 17: 1039–1068, 1994.

[15] F. Bernis, L.A. Peletier, and S.M. Williams. Source type solutions of a fourth order nonlinear degenerate parabolic equation. *Nonlin. Anal.*, 18:217–234, 1992.

[16] F. Bernis. Finite speed of propagation for thin viscous flows when $2 \leq n < 3$. *C. R. Acad. Sci. Paris Sér. I*, 322:1169–1174, 1996.

[17] F. Bernis. Finite speed of propagation and continuity of the interface for thin viscous flows. *Adv. Diff. Eq.*, 1:337–368, 1996.

[18] J. Hulshof and A. E. Shishkov. The finite speed of propagation property for the thin film equation in terms of the l^1-norm. *Adv. Diff. Equ.*, 3:625–642, 1998.

[19] F. Bernis, J. Hulshof, and F. Quirós. The 'linear' limit of thin film flows as an obstacle-free boundary problem. *SIAM J. Appl. Math.*, 61: 1062–1079, 2000.

[20] J. R. King and M. Bowen. Moving boundary problems and non-uniqueness for the thin film equation. Leiden preprint MI 28-99, to appear in Euro. J. Appl. Math., `http://www.cs.vu.nl/~jhulshof/PAPERS/bowen2.ps`.

[21] G. I. Barenblatt. *Scaling, Self-Similarity and Intermediate Asymptotics.* Cambridge University Press, 1996.

[22] F. Bernis, J. Hulshof, and J. R. King. Dipoles and similarity solutions to the thin film equation in the half-line. *Nonlinearity*, 13:413–439, 2000.

[23] J. Hulshof. A local analysis of similarity solutions of the thin film equation. *Nonlinear analysis and applications, Warsaw (GAKUTO Internat. Ser. Math. Sci. Appl. 7) (Tokyo: Gakkotosho)*, 7:179–197, 1994.

[24] M. Bowen and J. R. King. Asymptotic behaviour of the thin film equation in bounded domains. Leiden preprint MI 29-99, to appear in Euro. J. Appl. Math., `http://www.cs.vu.nl/~jhulshof/PAPERS/bowen1.ps`.

[25] D. G. Aronson and J.L. Vazquez. Calculation of anomolous exponents in nonlinear diffusion. *Phys. Rev. Lett.*, 72:348–351, 1994.

[26] J. Hulshof and J.L. Vazquez. Selfsimilar solutions of the second kind for the modified porous medium equation. *Euro. J. Appl. Math*, 5:391–403, 1994.

[27] N. Goldenfeld, M. Olivier, and Y. Oono. Intermediate asymptotics and renormalization group theory. *J. Sci. Comput.*, 4:355–372, 1989.

[28] G. J. B. van den Berg, J. Hulshof, and R. C. A. M. van der Vorst. Travelling waves for fourth-order semilinear parabolic equations. Leiden preprint MI 16-99, `http://www.cs.vu.nl/~jhulshof/PAPERS/43.ps`.

[29] L. Perko. *Differential Equations and Dynamical Systems.* Springer-Verlag, 1993.

[30] J. R. King. Integral results for nonlinear diffusion equations. *J. Eng. Math.*, 25:191–205, 1991.

[31] J. R. King. Two generalisations of the thin film equation. To appear.

[32] J.W. Cahn, C. M. Elliott, and A. Novick-Cohen. The Cahn-Hilliard equation with a concentration dependent mobility: motion by minus the Laplacian of the mean curvature. *Euro. J. Appl. Math.*, 7:287–301, 1996.